

# Analog Active Noise Canceling Headset

Electronic Design Lab - EE 318

Skand Hurkat, 08007013

Indrasen Bhattacharya, 08007032

Srujan Meesala, 08007036

Department of Electrical Engineering, IIT Bombay

May 3, 2011

## Abstract

Analog systems to achieve active noise cancellation in headphones were designed and implemented. Our project addresses two distinct techniques - feed forward and feedback systems. The work up to mid-semester, which was focused mainly on a feed-forward system with the motivation of developing a clip-on platform for generic earphones, is presented briefly. Limitations of this approach that lead to a poor noise cancellation figure (5-10 dB) are identified. Subsequently, feedback-based noise cancellation methods based on analog circuits as well as DSP are studied. As the central goal of this project, we focus on the design of an analog feedback control system based on cascade compensation. After identifying the plant frequency response, a suitable compensation network comprising lag and lead circuits was designed. In theory, the design aims to achieve a maximum noise cancellation of 20 dB at 100 Hz while simultaneously maintaining good stability margins, which are essential due to high plant variability. Circuits for implementing the compensator were designed and characterized. The performance of the entire closed loop system is then evaluated in terms of noise cancellation figures and frequency response of the music input. We achieved a maximum noise cancellation of 17 dB at 100 Hz and an improvement in the headphone response for bass inputs.



# Contents

<b>1</b>	<b>Introduction</b>	<b>3</b>
<b>2</b>	<b>Feed-forward active noise cancellation</b>	<b>4</b>
<b>3</b>	<b>Feedback active noise cancellation</b>	<b>6</b>
3.1	Motivation for analog feedback system . . . . .	7
3.2	Block Diagram for Analog Noise Control System . . . . .	9
3.2.1	Transfer Function . . . . .	10
3.2.2	Requirements in final system . . . . .	10
<b>4</b>	<b>Plant characterization</b>	<b>11</b>
<b>5</b>	<b>Primary compensation network</b>	<b>13</b>
5.1	Design requirements . . . . .	13
5.2	Lag and lead compensation . . . . .	15
5.2.1	Basic theory . . . . .	15
5.2.2	Inadequacy of simple lag . . . . .	15
5.3	Second order damped lag design . . . . .	16
5.3.1	Basic theory . . . . .	16
5.3.2	Design . . . . .	19
5.4	First order lag design . . . . .	19
<b>6</b>	<b>Circuit Design for Primary Compensation and System Testing</b>	<b>20</b>
6.1	Design of Mic Preamp . . . . .	20
6.2	Design of Active Second Order Lag System . . . . .	21
6.2.1	Sallen-Key Topology . . . . .	21
6.2.2	Kerwin-Huelsman-Newcomb (KHN) Biquad Filter . . . . .	21
6.2.3	Single Amplifier Biquad (SAB) Filter . . . . .	22
6.2.4	Tow-Thomas Biquad Filter . . . . .	23
6.2.5	Characterisation of the Tow-Thomas Biquad . . . . .	24
6.3	Design of Active First Order Lag/Lead Networks . . . . .	24
6.4	System testing and issues . . . . .	25
<b>7</b>	<b>Modified Compensation Network and System Testing</b>	<b>25</b>
7.1	Inclusion of LF lead and new HF lag . . . . .	26
7.2	The cascaded compensator and its characterization . . . . .	27
7.3	Evaluation of closed loop frequency responses . . . . .	29
7.4	Compensator for the right channel . . . . .	29
<b>8</b>	<b>Results and Discussion</b>	<b>31</b>
8.1	Noise Cancellation Response Measurements . . . . .	31
8.2	Music Response Characterisation . . . . .	32
<b>9</b>	<b>Conclusion</b>	<b>35</b>
<b>A</b>	<b>Right channel frequency response characteristics</b>	<b>38</b>
<b>B</b>	<b>SPICE simulation results</b>	<b>39</b>
<b>C</b>	<b>Complete circuit schematic</b>	<b>41</b>

# 1 Introduction

A noise-canceling headset and associated circuitry is aimed at reducing ambient noise and improving the musical experience of the user. Ambient noise is an external sound that impinges on the ears of the listener using headphones and masks the music. Typical noises include the noise of a bus in which the user is riding, or an AC machine running in a room. Many such continuous noise sources are at low mains-like frequencies of 50-100 Hz.

Often, headsets are built with padding/foam which passively reduce noise by mechanical damping. This is specially effective at high frequency external noise due to the mechanical low pass filtering action of such padding. Indeed, at high frequencies, we may have 10-20 dB of noise cancellation. But, passive noise cancellation may be insufficient at low frequencies - which are the frequencies of interest for external motor/locomotive/engine noise. A technique to deal with such low frequencies of external noise is **active noise cancellation**.

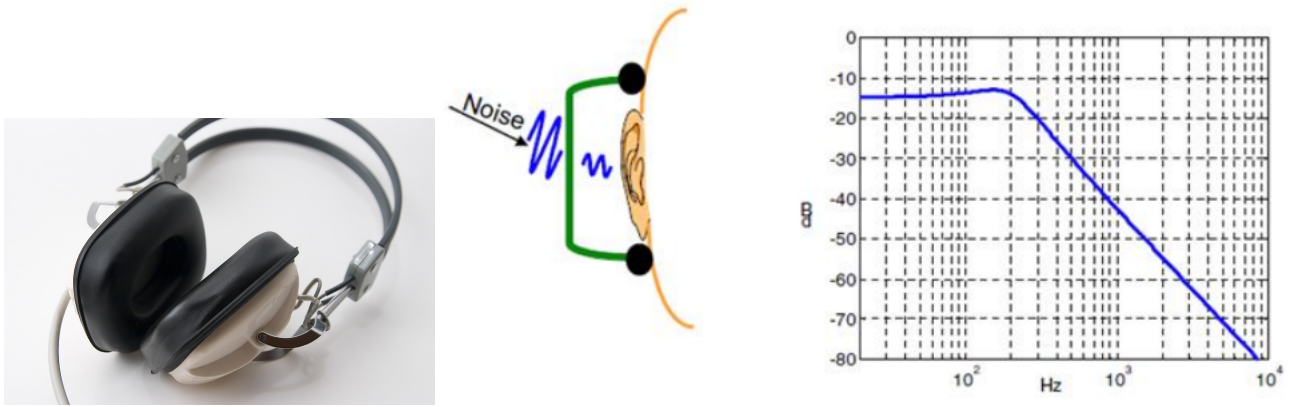


Figure 1: From L to R: Typical circumaural (full-ear covering) headphones, which provide substantial ambient noise cancellation at high frequencies (Fig. from [1]). A pictorial view of the passive attenuation of external noise provided by circumaural headphones (Fig. from [2]). A Bode magnitude plot of the simulated passive noise attenuation provided by such a headphone (Fig. from [2]). Note the low cancellation below 200 Hz.

Active noise cancellation involves the detection of external noise by suitable means and generating an equal and opposite signal to cancel out this external noise via **acoustic domain interference**. Several schemes are available for the generation of an antinoise signal. An external microphone may be placed for detecting the external noise, at a position close to the ear. An error-detecting microphone may be placed inside the setup, so as to detect the final signal entering the ear canal. The outputs from these transducers may be used in a systematic way to implement DSP-based algorithms such as the LMS algorithm. Another possibility is to implement a tracking control system which treats the music as an input to be followed and the external noise as a disturbance to the system. We are then interested in implementing a high **disturbance rejection**, which would effectively lead to noise attenuation. Some of the simplest active noise cancellation techniques depend on a direct feed-forward of the noise signal for generating an **anti-noise** signal. More complicated, but robust and better methods involve the use of feedback control systems implemented in the analog or digital domain, and even adaptive digital algorithms which lead to high active noise cancellation.

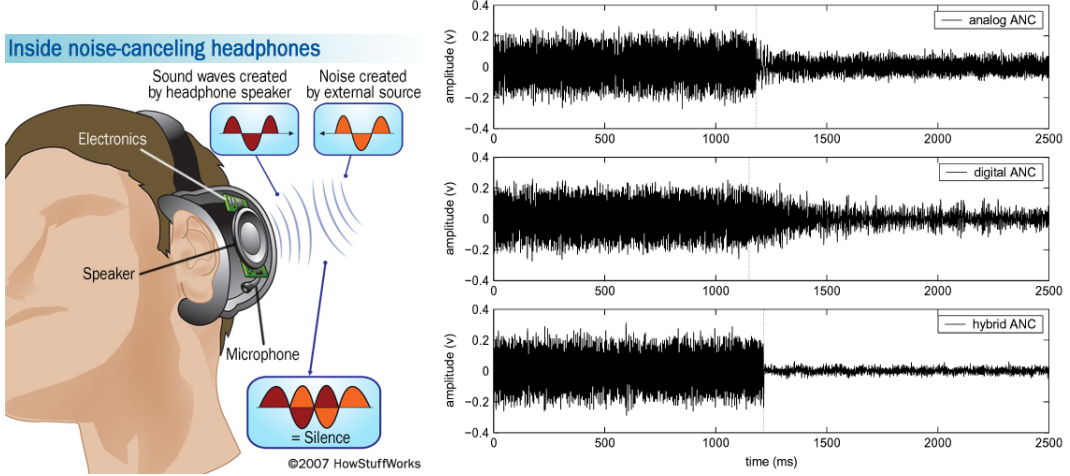


Figure 2: Left: Schematic illustrating the basics of active noise cancellation, with associated circuitry (Ref. [2]); Right: Three different time-domain noise cancellation graphs for analog, digital and hybrid noise cancellation systems - illustrating some of the most common issues with each of these. Analog noise cancellation is often not effective enough, whereas DSP-based noise canceling systems are slow. Hybrid systems combine the advantages of both (Ref. [3])

In this project, we implement two analog systems for active noise cancellation. The first system is a clip-on system based on feedforward active noise cancellation - which is supposed to be independent of the headphone setup to be used. We investigate the efficacy of this system and the dB level of noise cancellation obtained. Based upon our understanding of this feedforward system, and the nature of the noise, we later proceed to implement an analog feedback active noise cancellation system, based upon the system implemented in [4]. We shall first briefly discuss the feedforward system, and then proceed to a full description of the feedback system.

## 2 Feed-forward active noise cancellation

The basic idea of feed-forward active noise cancellation is just that of the detection of the external noise and feeding the inverted form of this in addition to the music to the headphone actuator. The basic idea is that of acoustic domain noise cancellation, and the expectation is that this will work out if the noise signal that is measured by the external microphone is close to the noise signal reaching the ear canal of the user. In the process, we make several simplifications which we shall detail further on.

The basic block diagram and the circuit schematic for this system is presented in Fig. 3 and Fig. 4. It essentially involves an inverted version of pre-amp output as anti-noise signal. The advantage of such a system is that there are no constraints really on the kind of headphone used, except that the distance between the external mic and the ear canal must not be too large, else we incur a delay which degrades performance. In order to obtain an understanding of active noise cancellation, we also tried out a few different configurations of the setup with a thermocol box to mimic the human head. Readings were taken to compare two cases of noise cancellation and noise amplification, with zero music. The readings are presented in the following pages.

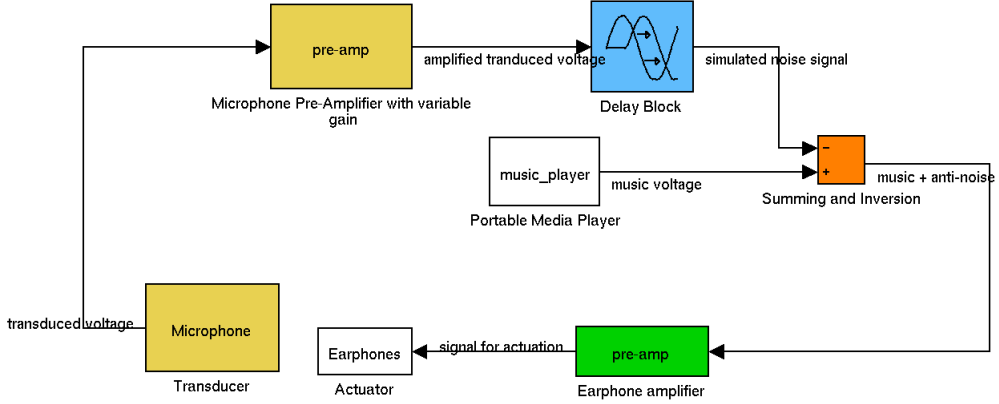


Figure 3: A functional description of the system, with the final output to the human ear being the output of the acoustic domain summation. The model includes a delay between the signal reaching the external mic, and the ear canal. Also, the mic-preamp gain could be adjusted by the user so as to allow for a good amount of noise cancellation. The music is just added at the actuator input.

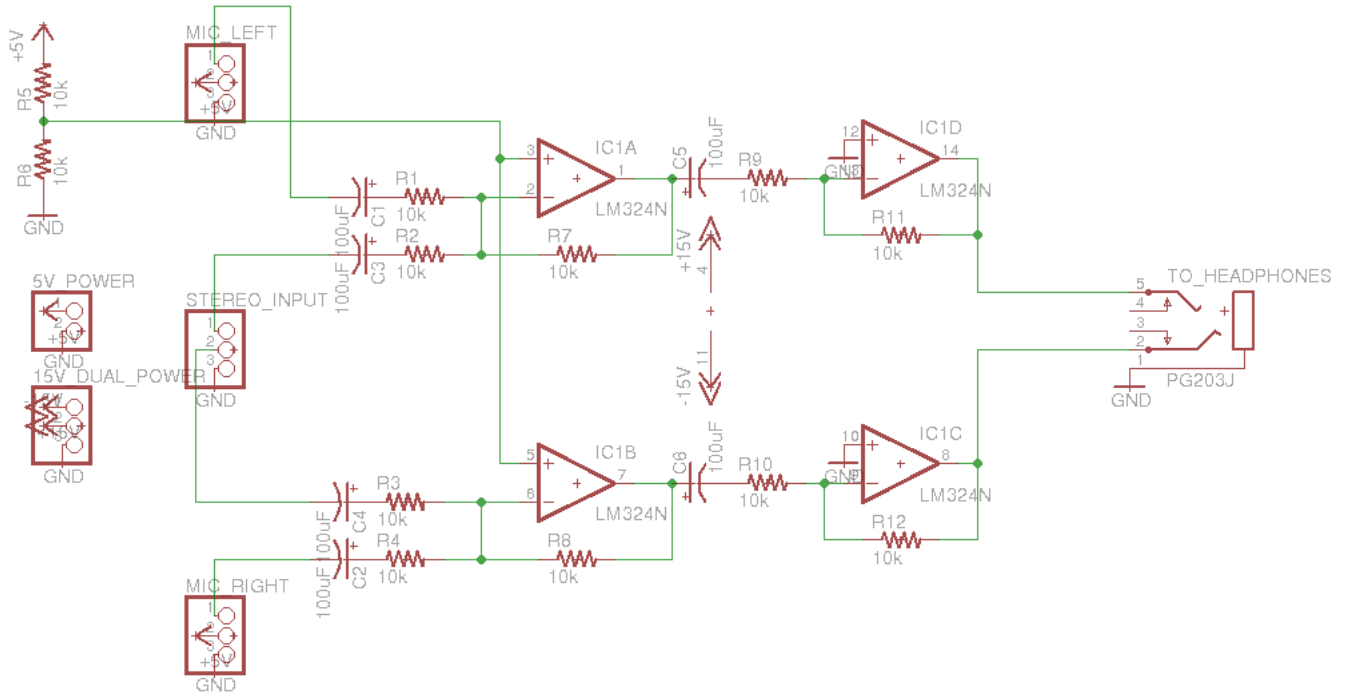


Figure 4: A circuit schematic of the feedforward system, showing the circuitry for each of the two channels.

To obtain the noise cancellation figure, and emphasize the difference due to active noise cancellation, we consider readings between two situations (Fig. 5). In the first situation, we play out the inverted noise signal, and this would lead to noise attenuation. In the second situation, we switch to the signal being directly fed, leading to acoustic domain addition, and thus amplification. The difference between the amplified and attenuated cases is quite marked.

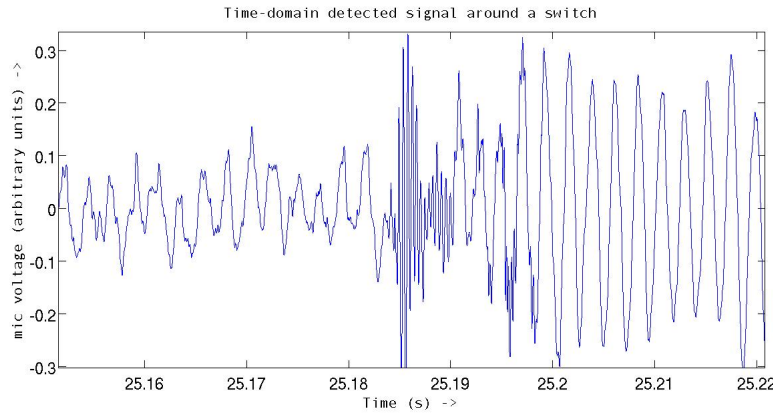


Figure 5: A tone of 440 Hz was played for this test. As can be seen, there is an attenuation of 10 dB (3 times) from amplifying to noise cancelling modes. Thus, the amount of noise attenuation provided is about 4-5 dB.

The amount of noise cancellation obtained turns out to be 4-5 dB for this direct feedforward system. There are several reasons for this kind of a degraded performance. Some of these reasons are highlighted below:

- **Delay:** There is a certain amount of delay introduced between the external sound reaching the microphone placed externally and the ear canal. Thus, whatever anti-noise signal is played by the headphone speakers is not exactly inverted, but is also out of phase. This phase difference tends to increase with the frequency of the external sound, leading to a performance degradation.
- **Direction of external noise:** The external microphone is placed at a point external to the headphone housing. It may happen that the external noise impinges on the setup in such a way that the noise actually detected by the external mic, and that reaching the ear canal are markedly different. This might happen if the source is not infinite (if it is close by), or if the position of the source keeps changing. Also, the effect of the headphone housing would alter the sound reaching the ear canal vis-a-vis the sound reaching the external mic. This issue would also lead to a mismatch between the noise and anti-noise signals.
- **Manual Control:** The system depends upon the user changing the microphone pre-amp gain in order to obtain just the right amount of cancellation. This is highly undesirable, as the user would need to keep changing this gain if the loudness of the external source were to be varying even gradually. Also, a mismatch in the mic pre-amp gain and the external noise level can actually lead to a worsening of performance even over the normal case. This motivates us to look at methods of **automatic control** which do not depend upon user feedback to correct for a mismatch in the gain of the circuitry.

The feedforward paradigm does not explore the possibility of detecting the error signal impinging at the ear canal and taking control actions to make sure that the external disturbance is rejected. One major issue with having to detect the error signal is that a transducer would have to be placed inside the housing of the headphone. There are a few difficulties with placing a microphone inside a headphone setup so as to detect the error due to the external noise. We conclude that the mic would have to be attached firmly with the body of the headphone amplifier so as to prevent mechanical variations - which could lead to sudden variations in the system. We will see how we can implement a feedback active noise cancellation system, and the major advantages provided by such a control philosophy in the next section.

### 3 Feedback active noise cancellation

A passive cancellation of 20 dB is already provided at high frequencies by the housing of the circumaural headphones. In order to achieve something of a similar level at the low-frequency range (100-500 Hz),

we require a noise cancellation level of **12-20 dB** from the active noise cancellation setup, significantly greater than the level provided by analog feedforward. Commercial headphones provide a stated noise cancellation level of upto 12-32 dB (Ref. [5]).

### 3.1 Motivation for analog feedback system

One of the major problems that we encountered with the feedforward system was that the manual control was unreliable and led to difficulties in the use of the system. Also, the level of noise cancellation provided is also quite low. There are several techniques to make things ‘automatic’ for the user. Such techniques include the use of different microphone placements to obtain data about the external signal and the error signal. The use of discrete time signal processing algorithms such as the **Least-Means-Square** algorithm and other adaptive techniques for noise cancellation implemented on DSP chips are quite prevalent.

There are three basic categories of noise cancellation systems as far as implementation goes. **digital** systems are more versatile and often lead to better noise cancellation. They allow a greater degree of freedom, and algorithms like LMS allow active noise cancellation which is optimal in a certain sense. The problem with digital systems is that they are often quite **slow** and require training sequences to find the ideal filter coefficients for the adaptive filter. If the system is to change, as is often the case for the headphone/ear-cavity system, we need a new training sequence for adjusting the filter weights. One way to circumnavigate this issue is to use the **recursive least means square algorithm** which updates filter weights on the fly - thus negating the necessity for new training sequences. But, this is at the cost of increased computational complexity for the adaptive filter, which leads to a greater delay. Thus, we find that digital systems are often *slow and sensitive to changes in the plant*.

On the other hand, **analog** systems are often fast and less expensive. Analog systems are dealt with in terms of automatic control theory, where the external noise is viewed as a disturbance to be minimised. Ref. [4], a patent by Amar Bose, provides a classical example of a closed loop system for active noise cancellation which manages to achieve a stated noise cancellation level of 20 dB. The headphone/ear-cavity system is treated as a plant to be controlled, and the open loop gain is increased as much as possible without compromising on the stability of the closed loop system. Bose’s circuit consists of a lead-lag compensator which achieves this requirement. We shall have a detailed look at this later. One major disadvantage of analog systems is that they do not allow us the freedom of designing filters to achieve an optimality criterion - such as *least means squares*. We are limited in scope by the practical issue of implementing analog domain transfer functions. Thus, the level of noise cancellation possible from analog systems is often lower than what is possible from digital adaptive filters.

The third and most effective category of noise cancelling systems are **hybrid** - in that they combine the robustness of analog systems and the optimality properties of digital systems. The analog system is used to make the plant more robust to changes in physical conditions. The digital system may then be used without sensitivity concerns because of the robust analog system built around the plant. A detailed discussion of a robust hybrid control system is presented in Ref. 3.

For our project, we have decided to narrow down on an analog system implementation in order to obtain a noise cancellation level between 12-20 dB. The reasons for our choice include the easy availability and low cost of components, the strong design and circuits component involved, which emphasize the suitability of this approach for an EDL project and the well established previous work in this field by Bose and others (Ref: 2).

The figures below from Ref. 6 are functional block diagrams for some of the common techniques used for active noise cancellation.

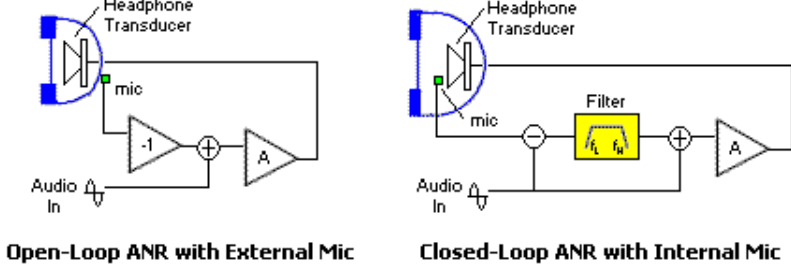


Figure 6: Left: A schematic of the feedforward system, with an externally placed mic. Right: An analog feedback system, with an in-housing mic which is used to feedback the error signal.

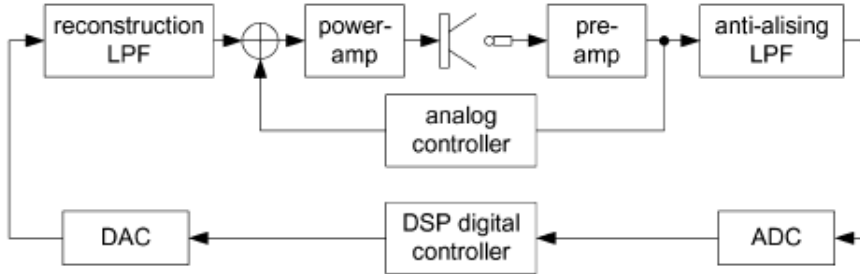


Figure 7: A hybrid system, with an analog system built around the plant so as to reduce the plant variations seen by the external digital system.

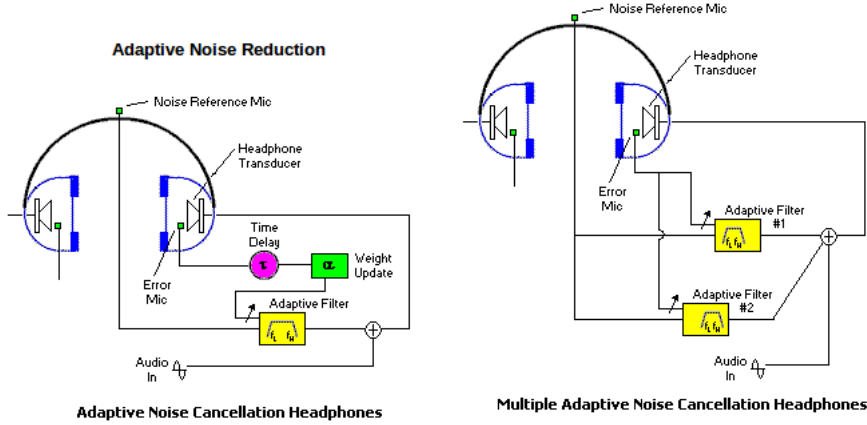


Figure 8: Left: An adaptive filter with fixed weights applied to the error mic output. Right: Schematic for a recursive LMS system with adaptive weights.

As a part of our midsemester goals, we had made a simplistic feedforward system which could be clipped on, and was essentially independent of the headphones used. But, the user would have to manually adjust the pre-amp gain in order to obtain the best possible performance that could be obtained. We were faced with several issues with the placement of the clip-on platform. The performance of any such system would have to be **robust** enough to deal with variations in the position of the clip on mic. Also, we would require the clipping to be extremely robust and resistant to mechanical wear and tear. Even if we were to make sure that this is the case, the maximum amount of cancellation that we could get would be limited to 5-6 dB, which is a constraint imposed on pure feedforward systems due to the absence of error feedback.

Thus, we finalized on a *non clip-on system* which would have the microphone placement integrated with the headset. In our new feedback setup, the headphones are an integral part of the system and

may be used to obtain a good system. We ensured that the headphones are circumaural so that the passive attenuation of higher frequencies is quite high. This would then match very well with the attenuation introduced by the active noise cancellation system at low frequencies - leading to an overall quieting effect. We chose “i-ball rocky” circumaural headphones with an impedance of  $32 \Omega$ , and with a frequency range of  $20 - 20000$  kHz in order to implement our noise cancelling headset. This was quite cheap (lesser than Rs. 500) and was giving a perceptible passive attenuation.

### 3.2 Block Diagram for Analog Noise Control System

In the implementation of a noise canceling system through analog circuits, we view our system in terms of the convention of automatic control theory. Our goal is to ensure that the sound reaching the ear canal continuously tracks the music that is input to the system, irrespective of the presence of an external disturbing noise. Thus, our objective is to build a **tracking control system** which follows the music and **rejects disturbances** of external noise. We may achieve this via the negative feedback of the output signal via a transducing microphone placed inside the housing of the headphones. A schematic block diagram is presented below:

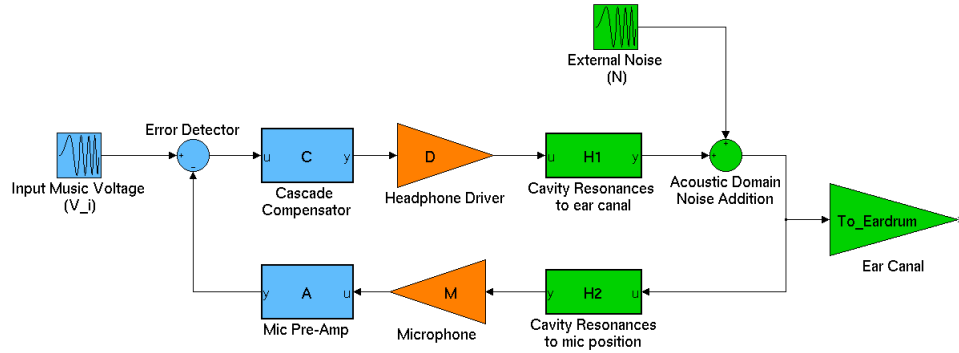


Figure 9: A schematic diagram of the complete control system. Key: blue - electrical domain, orange - transducers between the electrical and acoustic domains, green - acoustic domain. We see that this is a classical negative feedback system with cascade compensation. This topology is based upon the system implemented in Ref. 2.

The input is the voltage signal fed from the portable media player. This is what needs to be tracked. For our purposes, the output is the acoustic signal fed to the ear canal. A brief explanation of the various blocks (some of which are commonly used in controls parlance) is:

- **Error detector:** This is the block that subtracts the mic pre-amp output from the music to be tracked.
- **Compensator(C):** This is the linear system, with some transfer function, which ensures that the system has the desired closed loop characteristics. This may be implemented via various control techniques, which we shall soon examine.
- **Headphone driver(D):** The transducer that converts the electrical signal to mechanical vibrations.
- **Cavity Resonances(H<sub>1</sub>,H<sub>2</sub>):** This models the behaviour of the headphone/ear-cavity resonators, with respect to different positions inside the ear cavity (entrance of the ear canal, mic pre-amp position).
- **Microphone(M):** This is the output transducer, which converts the mechanical vibrations in the acoustic domain, to a low voltage electrical signal.
- **Mic Pre-Amp (A):** This is the amplifier which magnifies the voltage output of the mic to a level suitable for processing.

- **Plant (P):** The part of the system which is not explicitly under our control, which is characterised suitably and the compensator designed on the basis of that. For our design, we would choose to club together several of the blocks and characterize this combined block as the plant.

### 3.2.1 Transfer Function

Let the input from the portable media player be  $V_i(s)$  and the external noise(disturbance) be  $N(s)$ . Let the output pressure signal at the ear canal be denoted as  $L(s)$ . The transfer functions are denoted using their corresponding symbols as defined above. Then, the equation around the loop is:

$$L(s) = (V_i(s) - AMH_2L(s))DH_1C + N(s) \quad (1)$$

Thus, the closed loop transfer function for the music is:

$$G_{CL}(s) = \frac{L(s)}{V_i(s)} = \frac{DH_1C}{1 + AMH_1H_2CD} \quad (2)$$

and for the noise:

$$R_{CL}(s) = \frac{L(s)}{N(s)} = \frac{1}{1 + AMH_1H_2CD} \quad (3)$$

It turns out that the plants of  $H_1$ ,  $H_2$  are present together in the final expressions as the ‘plant’:

$$P(s) = AMH_1H_2D \quad (4)$$

which consists of the part of the open loop system between the headphone driver and the mic pre-amp. Later on, we shall see that it turns out to be quite convenient to completely ignore the acoustic domain behaviour, and look at the entire system between the driver and the mic pre-amp as a plant to be controlled. In terms of this plant transfer function, our various transfer functions turn out to be:

$$\text{Music Open Loop Transfer Fn.} = G_{OL}(s) = DH_1C \quad (5)$$

$$\text{Music Closed Loop Transfer Fn.} = G_{CL}(s) = \frac{DH_1C}{1 + PC} \quad (6)$$

$$\text{Noise Closed Loop Transfer Fn.} = R_{CL}(s) = \frac{1}{1 + PC} \quad (7)$$

$$\text{Open Loop Gain} = CDH_1H_2MA = CP \quad (8)$$

It is now quite clear why we define and work with the system  $P(s)$ . Also, another advantage is that this system has electrical input as well as output, thus negating the requirement for sensitive acoustic domain instruments to measure sound levels. Thus, we may proceed with an electrical interface in order to characterise what we call the ‘plant’ and then design a compensation network around that. But, in the process, we are sacrificing on our ability to change the mechanical setup so as to obtain advantages in the system design.

### 3.2.2 Requirements in final system

We shall now briefly recap our final goals in the control system design so as to keep things in perspective. The requirements of the final closed loop system can be expressed in terms of the following:

- **High Open loop gain:** If we have a high gain value in the frequency range of interest, we see that the noise closed loop transfer function goes lower, leading to a better amount of noise cancellation. Also, we would require the closed loop transfer function with respect to the music signal to be almost constant, in order that the system faithfully tracks the input music. This would also happen if the open loop gain  $|PC(j\Omega)|$  is high, leading to a good music tracking. Thus we have incentives for maintaining a high controller gain.

- **Closed loop stability:** By the Barkhausen criterion, if we have that the round-loop gain is greater than 1 where round-loop phase is  $180^\circ$ , then we have closed loop instability. This would be highly undesirable as the user would get to hear a very high magnitude tone-like sound. This phenomenon is known as **howling** - and we would clearly like to keep gain low enough around the round-loop phase inversion points so as to avoid such instabilities.

Thus, we see that we have two fundamentally contradictory criteria - one of high open loop gain so as to promote high noise cancellation - another of limited open loop gain so as to maintain robust **gain and phase margins**. We shall see how this can be done and how this affects our bandwidth of noise cancellation.

## 4 Plant characterization

In the previous sections, we had a brief look at some common implementations of noise cancelling headsets, and narrowed down towards analog feedback noise canceling systems. We then had a look at a particular topology implemented by Bose (Ref. 2), and examined the goals of a possible control system design including a cascade compensator. The design process begins with identifying the plant in terms of its frequency response. The characterization results are presented only for the left channel. Right channel frequency response data can be found in Appendix A.

As in the previous section, we would like to treat the plant in purely electrical terms - looking between the headphone driver and the mic pre-amp output, so that we may conveniently obtain frequency characteristics. In the characterisation process, we include:

- **Headphone driver(D)** - which is simply an appropriate audio op-amp feeding a voltage to the headphone actuator
- **Cavity resonances( $H_1, H_2$ )** - the acoustic domain resonances that arise at certain frequencies due to the cavity formed between the pinna and the headphone
- **Microphone(M)** - an electret microphone with a certain polarity, which detects pressure variations inside the housing of the headphones and transduces them to voltages of the order of  $10\mu V$
- **Mic pre-amp(A)** - An op-amp based amplifier and DC blocker from Ref. 2. It amplifies by 6.6 times and is sufficient to provide a detectable output which can be measured by conventional DSO's accurately.

In order to obtain a correct estimate of the effect of cavity resonances, we ensure that the plant characterisation conditions match as closely as possible with the conditions of usage. Thus, during the characterisation process, the headphones were placed on the head of a person in the normal hearing condition. Tones of different frequencies and *sufficient intensity to mask over background noises* were fed to the headphone driver - and the final output was recorded on a computer via the mic pre-amp output. This was recorded as the final output - and the gains and phases of this were combined to yield a complete result. This was done for both left and right channels of the headphones. Note that the mic pre-amp just provides a gain, which can be adjusted for later. Thus, we fix on the mic pre-amp gain for a particular experimental characterisation and use that data later with the final pre-amp we design for by adjusting the gain of the plant.

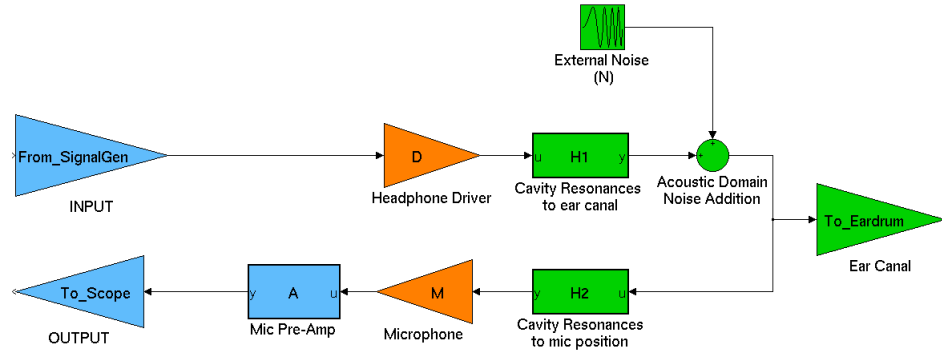


Figure 10: A schematic diagram for the connection of the blocks during the plant characterisation. We feed a pure tone from the signal generator to the cascade, measure the output from the mic pre-amp. Someone must be wearing the headset for an accurate simulation of the plant cavity resonances.

We carried out two characterisation runs of the plant, each time with a different person wearing the headset. We observe that there are marked variations in the frequency response of the plant with the different runs of the experiment. This is an important aspect of the system - it *depends sensitively on the headphone cavity* which is affected by the position of the headphones on the user's ears. The conclusion is that we must make sure that our compensation design is robust enough to meet even the worst case variations in the plant. This would be done by maintaining some gain and phase margins in the design.

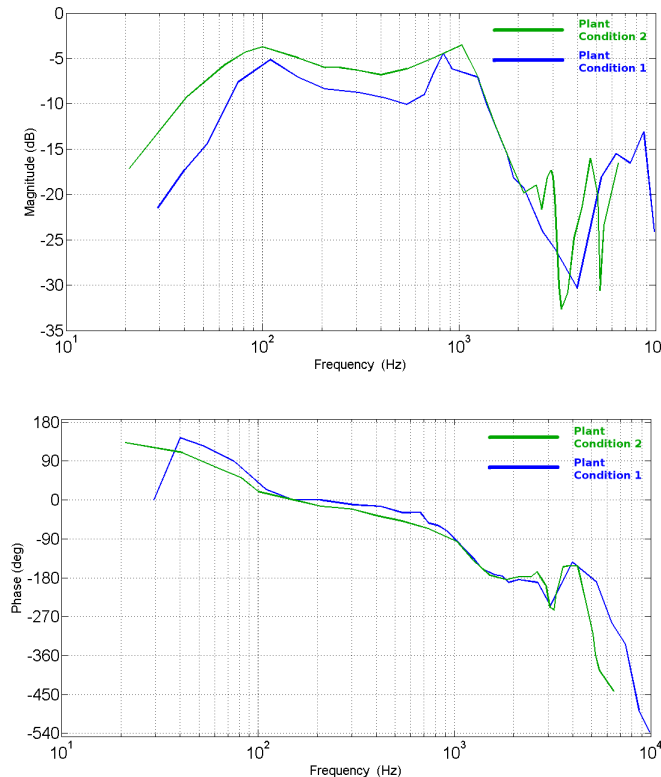


Figure 11: Figures corresponding to two different characterisations of the plant. top: The magnitude plots show variations in gain as well as the resonant cavity peaks; bottom: the phase response. We observe that there are marked changes in the plant being characterised due to changes in the ear cavity.

Having seen the phase and magnitude plots for the plant, it might be helpful to understand some of the components of the plant - so that we may design a compensator based upon this qualitative understanding. So, the salient frequency characteristics are summarised below:

- **Time Delay:** Between the actuator signal being played out and the microphone detecting the same, there is expected to be a roughly constant time delay due to the physical separation between the mic and the actuator. This leads to phase falling linearly without constraints as frequency is increased further - and contributes to the signal reaching  $-180^\circ$  rather fast. The presence of delays leads to special difficulties in control systems.
- **Low pass filtering:** Though the response of the headphones is stated to be 20 Hz to 20 kHz, we note that the gain of the headphones would start rolling off at a certain frequency due to the nature of the physical actuator. Also, a number of resonances are observed at certain frequencies above 3-4 kHz. These may possibly due to the diaphragm of the speaker being excited at these frequencies.
- **Cavity Resonances:** There are pronounced resonances above 4 kHz which may possibly arise due to these frequencies being resonant in the cavity. Also, at these resonances, we have rapid changes in phase which would lead to phase crossover points being reached in relatively small frequency intervals. Thus, we would wish to keep open loop gain to be lesser than 1 at the frequencies where the resonances occur.

Keeping all these considerations in mind, we shall now focus on the systematic design of a control system to achieve our stated requirements.

## 5 Primary compensation network

### 5.1 Design requirements

The basic purpose of the cascade compensator is to shape the transfer function of the system in the forward path so as to achieve a *stable closed loop system* at a *large open loop gain*, which is required to achieve disturbance rejection and input following. A broad outline of the compensator design process is as follows -

1. Fix a certain desired noise cancellation level as an initial design specification, and calculate the forward path gain required to achieve the same.
2. From the Bode plot of the plant with increased gain, identify the gain and phase crossover points. Using these points as a starting guideline for potential howling frequencies, design a compensator to achieve suitable stability margins. In our case, we aim to achieve gain margins greater than 5 dB and phase margins greater than  $30^\circ$ .
3. With the compensator thus designed, compute the resultant closed loop responses for music and noise. Verify if the noise cancellation specification is met and the music response is *better* than that of the uncompensated plant.

In the part of the report that follows on compensation design, we consider the left channel plant. The right channel compensation design is dealt with in a subsequent section, and as we shall see, we can retain the design made for the left channel almost entirely. From the plant characteristics (Fig. 4), we observe that the magnitude response is maximum and reasonably flat over the 100 Hz - 1 kHz range (between -5 dB and -10 dB). At frequencies above and below this range, the plant gain rolls off and poses a fundamental limitation to the amount of noise cancellation that can be achieved. We therefore set our **target cancellation bandwidth to the 100 Hz - 1 kHz range**.

For the purpose of plant characterization, the mic pre-amp gain was chosen arbitrarily so as to allow us to obtain a reasonably large voltage output (100s of mV). We now adjust this gain so as to achieve approximately 0 dB gain over the cancellation bandwidth. This is done in order to normalize the open loop plant response so as to facilitate easy design. So the mic-preamp gain is increased by a  $2 \times$  (6 dB) factor to add to the existing -5 dB. We now design our compensator around this yanked plant, which we shall refer to as the plant hereafter.

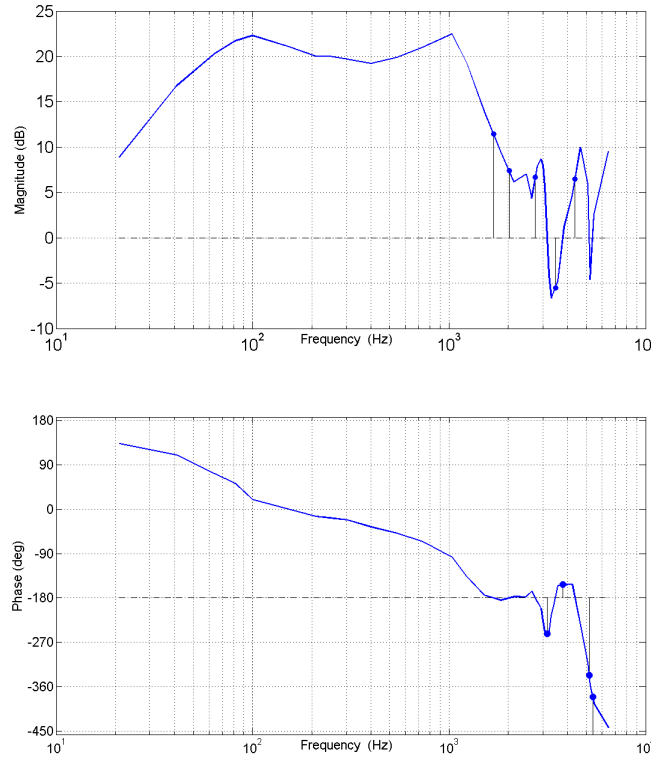


Figure 12: Bode magnitude and phase response of plant with a gain of 20 dB. The circled points indicate the gain and phase crossover frequencies.

1. The noise cancellation figure is defined by the closed loop transfer function ( $R_{CL}(s)$ ) for the noise signal. We fix a **noise cancellation level of 20 dB at 100 Hz frequency as an initial design target**. From (Eqn 7), assuming zero phase, this would require that at 100 Hz

$$1 + PC = 10 \quad (9)$$

Since the plant  $P$  has nearly 0 dB gain at 100 Hz, we get  $|C| \approx 9$ . **The compensator must therefore provide a gain of 25 dB at 100 Hz.**

2. We now consider the stability of the closed loop system with an added gain of  $10 \times$  (20 dB). Fig. 12 shows the Bode plot of the plant with a gain of 20 dB. It can be seen that the  $180^\circ$  phase and 0 dB crossover frequencies all lie beyond 1 KHz (Fig. 13). We identify the **region beyond 1 KHz as a potential instability region for the closed loop system**.
3. From the phase crossover frequencies, we observe that the maximum (and lowest) gain instability is at 1 KHz with a gain of 10 dB. In order to achieve a stable closed loop system, with a minimum gain margin of 5 dB, **the compensator gain must be at least as low as -25 dB at 1 KHz** with 100 Hz gain as a reference.
4. From the gain crossover frequencies, we observe that the plant already has good phase margins within  $30^\circ$ . The compensator must therefore continue to maintain phase margins within the  $30^\circ$  limit by ensuring that its **phase beyond 1 KHz is preferably zero or positive**.
5. While designing the compensator, we must always bear in mind the **tradeoff between cancellation bandwidth and stability margins**. Cutting down on gain at 1 KHz and beyond would inevitably reduce the gain in the cancellation bandwidth as well. We must ensure that the 20 dB cancellation spec at 100 Hz is not violated in the process of compensator design.

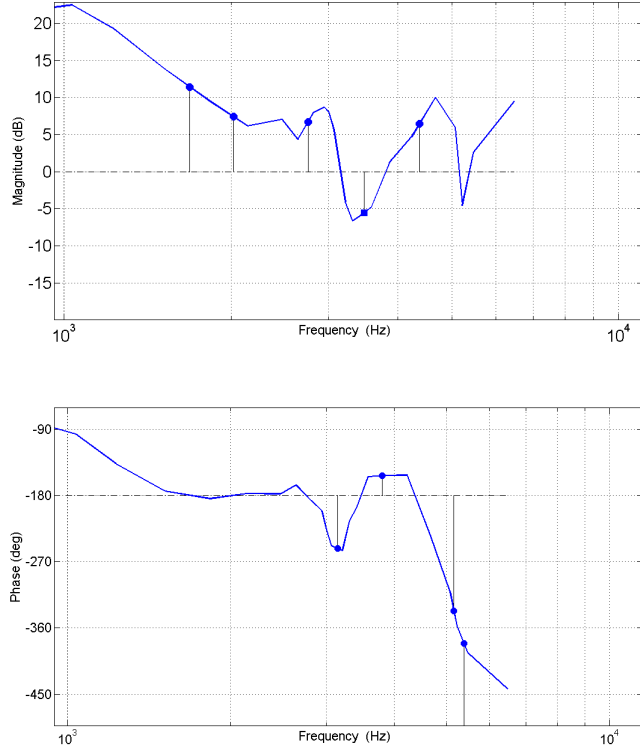


Figure 13: Bode magnitude and phase plots of plant zoomed in over potential instability region (beyond 1 KHz).

## 5.2 Lag and lead compensation

### 5.2.1 Basic theory

The design requirements arrived at above demand that we achieve a rise/fall in gain over certain prescribed frequency regions with a corresponding local variation in phase. This is different from the responses of filters, which typically roll off continually in gain and add permanent phase changes. Lag and lead networks are commonly used to shape open loop frequency response characteristics to achieve stable feedback systems. The basic (first order) lag/lead transfer function structure is

$$H(s) = K \left( \frac{s + \omega_z}{s + \omega_p} \right) \quad (10)$$

For a lag system, the denominator frequency  $\omega_p$  *lags* the numerator frequency  $\omega_z$  ( $\omega_p < \omega_z$ ). While for the lead system,  $\omega_p > \omega_z$ . Considering the lag system as an example, we observe that we can achieve

1. A stepped attenuation of  $\omega_z/\omega_p$  achieved gradually over the range  $(\omega_p, \omega_z)$
2. A negative phase over a range defined roughly by  $(0.1\omega_p, 10\omega_z)$ , which dips in between and levels off to zero outside this range.

Similarly, the lead system achieves a stepped increase in gain and a positive phase over the range  $(\omega_z, \omega_p)$ .

### 5.2.2 Inadequacy of simple lag

Our compensation design problem requires **effectively a lag for the frequencies beyond 1 KHz** in order to reduce the gain. However, the phase dip must not be so large that phase margins are reduced. Further, the transition range for the magnitude response must not be too broad or the cancellation

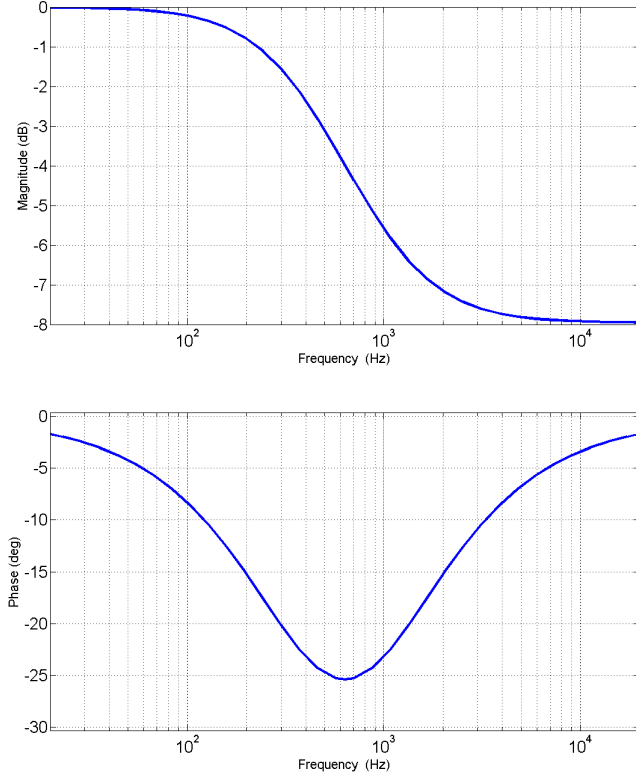


Figure 14: Bode plot of lag 1 achieved with the transfer function  $H(s) = 0.4(s + 2\pi 1000)/(s + 2\pi 400)$ . This compensator does not stabilize the closed loop system.

bandwidth would have to be compromised. Figs. 14, 15 show possible designs of a lag compensator for our plant, which illustrate extremes of these two cases.

1. In Fig. 14, the gain at 100 Hz is not compromised (kept close to 0 dB) so as to maintain the initial noise cancellation spec. However, the gain achieved at 1 KHz is about -6 dB and is insufficient.
2. In Fig. 15, the desired gain of -25 dB is obtained at 1 KHz. But this is achieved at the expense of a negative phase as large as  $-20^\circ$  in the potential instability region. Also the gain at 100 Hz is now reduced to -8 dB, thereby reducing the compensator+plant gain to 12 dB ( $4\times$ ). This would mean a noise cancellation of  $1/(1+4) \rightarrow 14$  dB, which is far from the initially desired spec of 20 dB.

Thus the simple first order lag is grossly inadequate as a compensator if we are to achieve the desired amount of noise cancellation. The possibility of using a cascade of two first order lags to realize a second order lag with a large gain dip is ruled out since this drastically affects the phase response by allowing phase dips exceeding  $90^\circ$ .

### 5.3 Second order damped lag design

#### 5.3.1 Basic theory

The inadequacy of simple and cascaded first order lag stages forces us to consider other options. The compensation design used in the patent by Bose (Ref. 2) relies on second order damped systems to realize lag and lead networks. On exploring the basic structure of the transfer function for such a system, we see that it indeed offers significant advantages. A second order damped lag compensator has a transfer function of the form

$$H(s) = K \left( \frac{s^2 + 2\zeta_z \omega_z s + \omega_z^2}{s^2 + 2\zeta_p \omega_p s + \omega_p^2} \right) \quad (11)$$

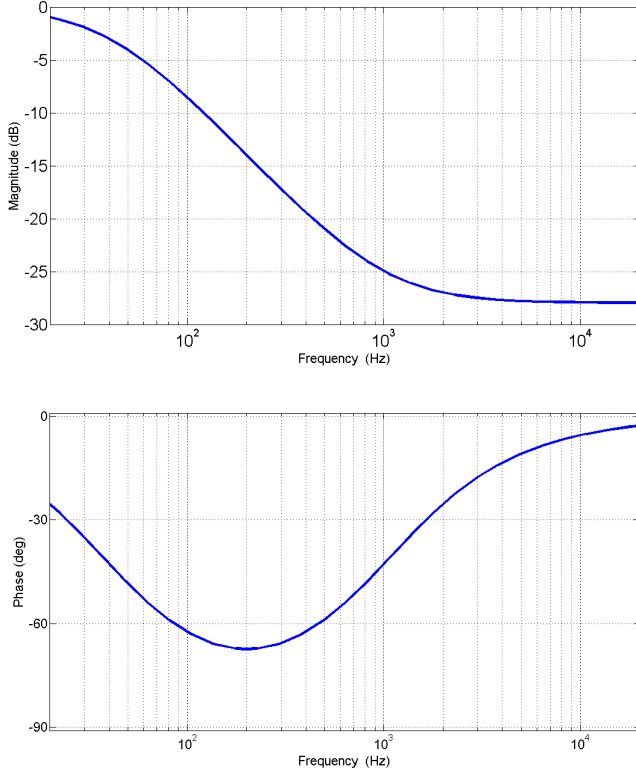


Figure 15: Bode plot of lag 2 achieved with the transfer function  $H(s) = 0.04(s + 2\pi 1040)/(s + 2\pi 40)$ . This compensator achieves poorer noise cancellation than desired.

where the damping ratios  $\zeta_z, \zeta_p < 1$  and  $\omega_z > \omega_p$ .

The frequency response would therefore be

$$H(j\omega) = K \left( \frac{(\omega_z^2 - \omega^2) + j2\zeta_z\omega_z\omega}{(\omega_p^2 - \omega^2) + j2\zeta_p\omega_p\omega} \right) \quad (12)$$

The overall low frequency to high frequency dB attenuation is determined by  $(\omega_z/\omega_p)^2$  and is twice as large as that offered by a first order system with same frequencies. More importantly, the presence of damped poles and zeros allows us to have a peak or a dip in the overall attenuating magnitude response due to the lag behaviour. We may understand this intuitively by considering the magnitude response of a system with just two damped poles and no zeros as shown in Fig. 16. It can be observed that with a decrease in damping ratio (i.e. more heavily damped poles), the gain before the pole frequency tends to peak even more.

For our system, we can therefore understand that we may expect a peak close to the pole frequency ( $\omega_p$ ) or a dip close to the zero frequency ( $\omega_z$ ) according as  $\zeta_p$  and  $\zeta_z$  are varied. Since we desire the latter for our compensator, we use a lower damping ratio for the zeros than for the poles in the design that follows.

Another advantage of the damped second order system is that the phase response is not directly determined by the square of the frequency, which is the case with a cascade of first order lags. Furthermore, the damping ratios  $\zeta_z, \zeta_p$  also serve as tuning parameters for the phase response. In fact, choosing  $\zeta_z, \zeta_p$  appropriately allows us to achieve a *positive going phase at frequencies higher than  $\omega_z$* . Again this maybe understood by considering the behaviour of the phase response of the simple second order damped system in Fig. 16.

The second order damped lag system may therefore be used to achieve a *dip in the magnitude*

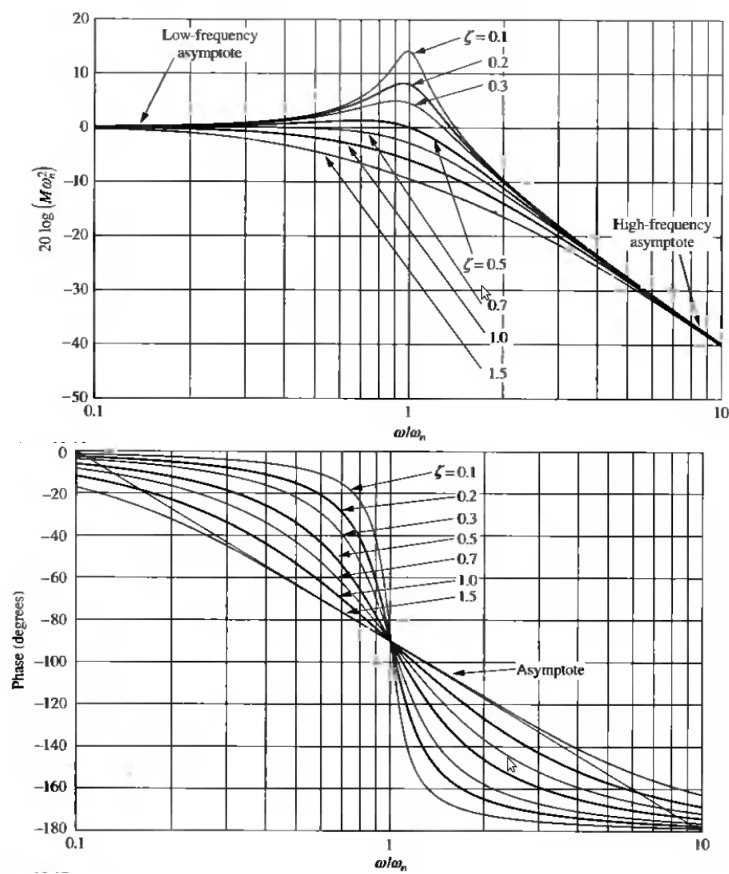


Figure 16: Normalized magnitude and phase responses of a second order damped system  $1/(s^2 + 2\zeta\omega_n s + \omega_n^2)$  for fixed  $\omega_n$  and varying values of damping ratio  $\zeta$ . Figs. from [9]

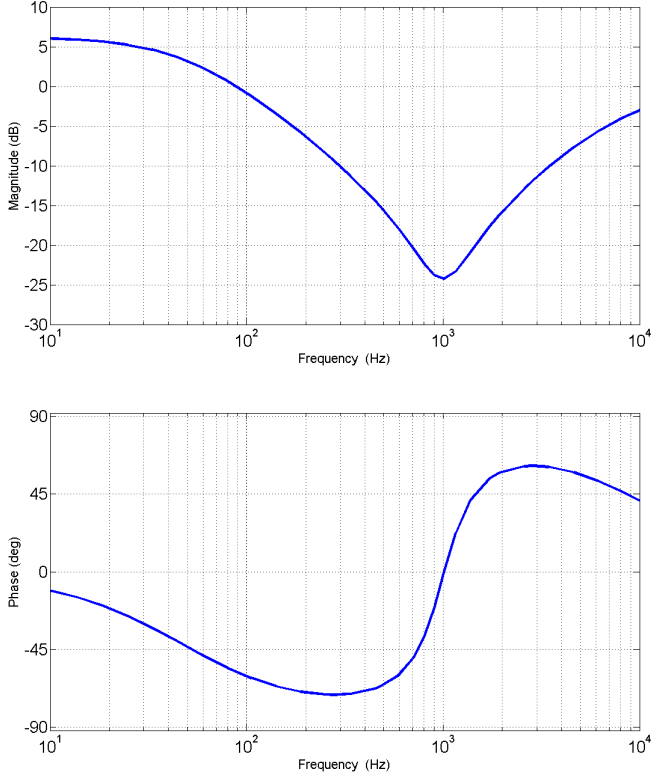


Figure 17: Bode plot of second order damped lag compensator designed to sharply shape the frequency response at 1 KHz.

*response close to 1 KHz, which can be immediately followed by a sharply rising phase.*

### 5.3.2 Design

1. Since we must design for a maximum gain dip at 1 KHz, we set the numerator frequency  $f_z = 1$  KHz
2. The denominator frequency is chosen at  $f_p = 700\text{Hz}$  so as to achieve a 25 dB attenuation at 1 KHz compared to the gain at 100 Hz.
3. Tune  $\zeta_n$ ,  $\zeta_p$  so as to achieve zero phase at 1 KHz. This ensures that we have only positive going phase beyond this frequency, thereby boosting the phase in the potential instability region. With  $\zeta_n = 0.3$ ,  $\zeta_p = 7$ , we achieve a peak phase dip of  $-70^\circ$  around 300 Hz and a maximum phase of  $55^\circ$  around 3 KHz. We note that reducing the phase below 1 KHz is not an issue since these frequencies have a phase response significantly above  $-180^\circ$ .
4. The transfer function of the system thus achieved is

$$H(s) = \frac{s^2 + 0.6(2\pi)(1000)s + ((2\pi)(1000))^2}{s^2 + 14(2\pi)(700)s + ((2\pi)(700))^2} \quad (13)$$

The Bode plot of the system thus designed is presented in Fig. 17.

### 5.4 First order lag design

With the second order damped lag designed above, we have achieved the desired -25 dB dip at 1 KHz, which is the maximum gain instability frequency as seen earlier. The attenuation offered by this system at higher frequencies (-10 dB at 3 KHz) is not sufficient to achieve gain margins of at least 10 dB. We therefore consider placing a simple first order lag to achieve extra attenuation at these frequencies. The

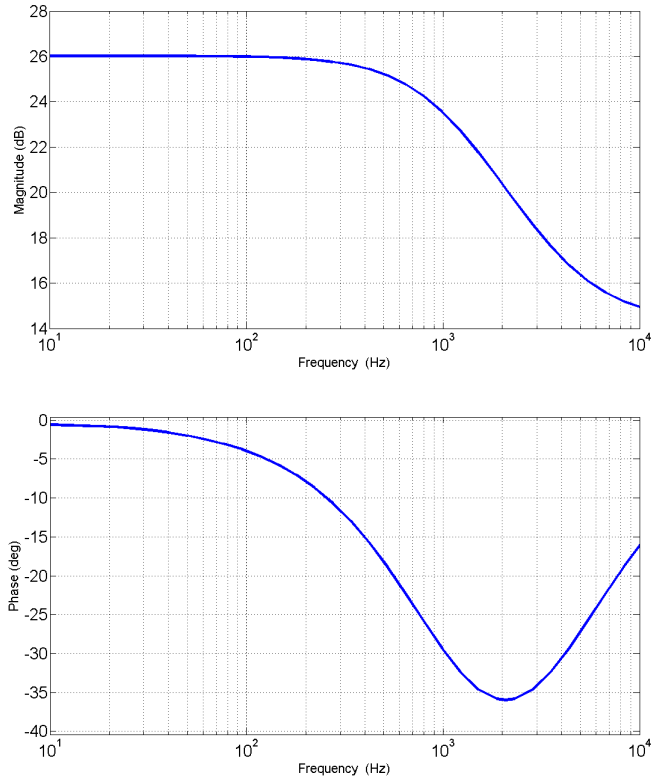


Figure 18: Bode plot of first order lag designed to lower gain at frequencies beyond 1 KHz

positive phase added by the damped lag network designed above provides us with some advantage in that we may design this new lag with a little less concern about its negative phase contribution.

The pole frequency for this network is chosen as  $f_p = 1$  KHz. The zero frequency is then adjusted to the extent that the phase margins are not compromised. With this approach, we arrive at  $f_z = 4$  KHz. This gives us an attenuation of around 7 dB at 3 KHz. The resulting transfer function is given below and the Bode plot is shown in Fig. 18.

$$H(s) = \frac{0.00078s + 20}{0.00015s + 1} \quad (14)$$

## 6 Circuit Design for Primary Compensation and System Testing

### 6.1 Design of Mic Preamp

We use an electret mic in the project. An electret mic is a low-cost easily available solution, with a good response. The electret mic provides a small signal riding on a DC offset. To get rid of the DC offset, we need to add DC blocking capacitors at the input of the mic preamplifier. However, we do not want phase to be affected greatly by the presence of the DC blocking capacitors, and want the gain of the mic preamp to be uniformly flat over the frequency band of interest, namely 20Hz to 20kHz.

Hence, a high-pass filter with a low frequency was chosen. The cutoff frequency of the high pass filter was chosen to be 0.338Hz. This ensures good DC blocking with a flat response over the frequency band of interest. Further, the output of the passive filter was connected to a non-inverting amplifier with a high gain.

The gain of the mic-preamplifier was chosen thus:

We put in an arbitrary gain of 6.6 in the mic preamp and characterized the plant. Then we saw how much lower the plant magnitude was in comparison to the 0dB line, and the gain of the mic preamp was adjusted accordingly so as to bring the gain of the uncompensated plant from 100Hz to 1kHz to

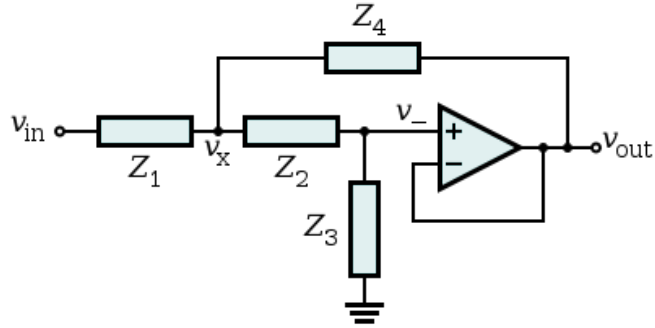


Figure 19: Sallen-Key Topology for a Second Order Filter

near 0dB. Hence, we found out that we needed a gain of 11 in the left channel and a gain of 17.5 in the right channel.

Choosing gains in this manner ensured that we would have the response of the compensated headphones would be as close to that of the open-loop response, as in, we would have the same sound pressure levels in the ears for the same input, and also that we would prevent over-driving the headphones.

## 6.2 Design of Active Second Order Lag System

The given second order lag function is  $\frac{s^2 + 0.6 \times 2\pi 1000 + (2\pi 1000)^2}{s^2 + 14 \times 2\pi 700 + (2\pi 700)^2}$ . What we immediately notice is that the numerator has complex conjugate roots. This makes the design of the Lag system challenging, because it cannot be made from cascade of familiar first order systems.

We considered many different topologies for the design of the second order lag system. The following is a brief discussion about the options considered.

### 6.2.1 Sallen-Key Topology

Sallen-Key filters are extremely popular because of their simplicity. They are widely used to achieve implementations of second order systems, and hence we decided to try and implement our system on a Sallen-Key topology.

The Sallen-Key topology is shown in 19. The transfer function of this filter is

$$T(s) = \frac{v_{\text{out}}(s)}{v_{\text{in}}(s)} = \frac{Z_3 Z_4}{Z_1 Z_2 + Z_4(Z_1 + Z_2) + Z_3 Z_4} \quad (15)$$

We shall use only capacitors and resistors in the design. Inductors shall not be used primarily because of low reliability. We consider each  $Z_i$  to be a composite, i.e. it contains either a series or a parallel combination of resistors and capacitors, so that either  $Z_i = R_i + \frac{1}{sC_i}$  or  $Z_i = \frac{R_i}{sC_i R_i + 1}$ .

What we notice with this topology is that complex roots are not possible, because the numerator of the transfer function hence formed can always be decomposed into a product of linear polynomials with real roots.

This discounts the possibility of using a Sallen-Key topology for implementing the second order lag network, which is an essential part of the compensation.

### 6.2.2 Kerwin-Huelsman-Newcomb (KHN) Biquad Filter

A KHN filter is a wonderful state variable filter. Any LTI system can be represented in state space form, and can be simulated using integrators, adders and gain blocks. A KHN filter uses this principle and can simultaneously produce high-pass, band-pass and low-pass outputs using three op-amps. These may be combined (added) using carefully chosen weights and hence we would obtain the required transfer function. The topology of the KHN filter is shown in 20.

The term biquad means that the filter realizes a system which contains a quadratic in the numerator as well as in a denominator. While a state variable filter seems a good and easy option for implementing

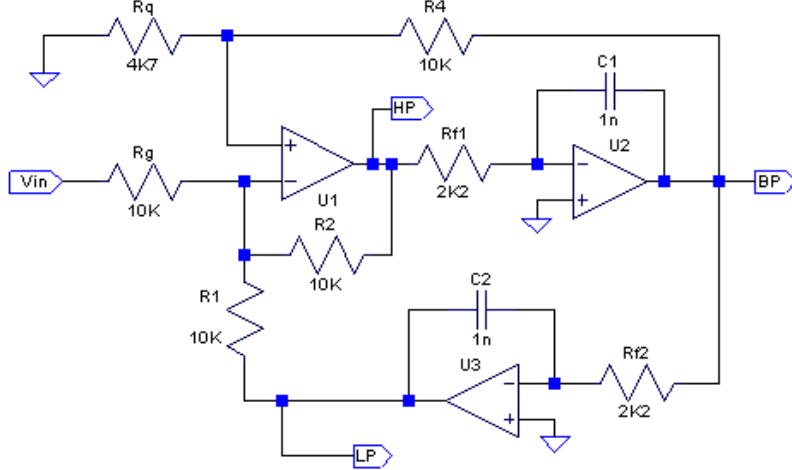


Figure 20: A KHN Biquad State Variable Filter

the desired transfer function, it requires a large number of op-amps for its implementation. While this may seem tempting in a lab environment, it is not a good option for a product, as a large number of amplifiers increase cost, power consumption and size.

In the KHN filter, it is intuitive to check that the output of the band-pass filter shall be inverted with respect to the output of the low-pass and high-pass filters. This means that in addition to the three op-amps required to implement the KHN filter, we shall need another op-amp for implementing an inverter and yet another for implementing an adder. Moreover, the weights attached to the adder are extremely sensitive to resistor values, and in general, would not give a stable design in the presence of unfavourable resistor tolerances.

### 6.2.3 Single Amplifier Biquad (SAB) Filter

Looking up biquad filter designs on the internet led us to the design of the SAB filter presented in [7]. The topology of the SAB filter is shown in 21. The transfer function of the filter is given by

$$T(s) = \frac{V_o(s)}{V_i(s)} = -\frac{fs^2 + \frac{g}{T}s + \frac{b}{T^2}}{s^2 + \frac{ad}{T}s + \frac{1+a(2+b)}{T^2}} \quad (16)$$

where

$$b+2 = g+e \quad (17)$$

$$f+2 = d \quad (18)$$

$$T = RC \quad (19)$$

As always, we find issues with this filter topology too. Though it seems that this topology can easily suit our needs, and can be used to make arbitrary biquad filters, that is not the case. We have a total of 8 parameters<sup>1</sup> to be chosen, and 8 constraints<sup>2</sup> between the parameters, as such, we do not have any degrees of freedom in being able to implement arbitrary biquad transfer functions.

On computing the required parameters for the given transfer function, we found out that  $f = 1.3 \times 10^{-3}$ .  $f$  is directly related to the gain of the SAB filter. What this means is that the SAB filter shall have very low gain. While this may not seem to be a major issue, considering that we may add an amplifier after this filter to restore the gain; the issues is more serious than meets the eye. At low gains,

<sup>1</sup>We need to be able to choose  $a$ ,  $b$ ,  $C$ ,  $d$ ,  $e$ ,  $f$ ,  $g$  and  $R$

<sup>2</sup>There are 5 constraints relating the ratio of the coefficients in both numerator and denominator of transfer function, and another 3 constraints mentioned in 17 to 19

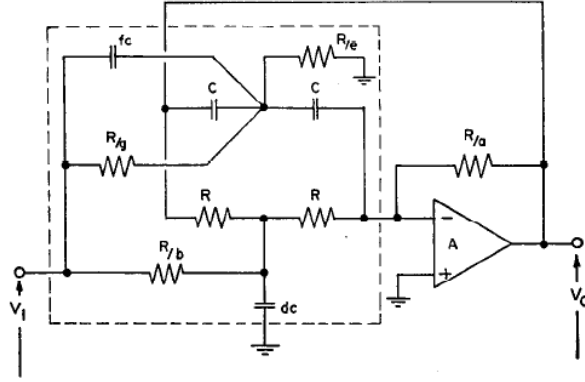


Figure 21: Single Amplifier Biquad Filter.

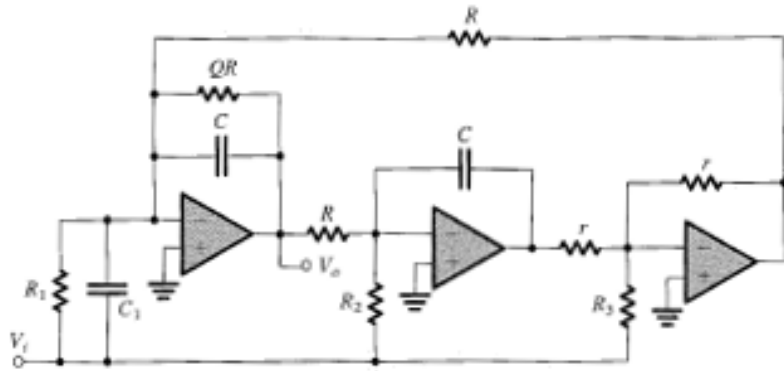


Figure 22: Tow Thomas Biquad Filter. Fig. from [8]

the inherent noise in the op-amp becomes comparable to the signal power at the output. This kills the signal-to-noise ratio (SNR). In a high-fidelity audio application like headphones, this is unacceptable.

This means that we cannot use the SAB topology, but must look for alternatives.

#### 6.2.4 Tow-Thomas Biquad Filter

The Tow-Thomas biquad topology is depicted in 22. It has a transfer function given by

$$T(s) = \frac{V_o(s)}{V_i(s)} = \frac{\left(\frac{C_1}{C}\right)^2 s^2 + \frac{1}{C} \left(\frac{1}{R_1} - \frac{r}{RR_3}\right) s + \frac{1}{C^2 RR_2}}{s^2 + \frac{1}{QR} s + \frac{1}{C^2 R^2}} \quad (20)$$

Finally, it seems as if we may achieve the circuit implementation of the desired transfer function. We want the gain of the filter to be unity, so  $\frac{C_1}{C} = 1$ , so  $C_1 = C$ . Further, we have  $\frac{1}{CR} = 2\pi 700$ , so we get  $RC$ . Further, we choose  $C = 33\text{nF}$  and  $R = 6800\Omega$ . We also have  $\frac{1}{Q} = 14$ , so we have  $QR = 485\Omega \approx 490\Omega = (270 + 220)\Omega$ . Further, we want  $\frac{1}{C} \left(\frac{1}{R_1} - \frac{r}{RR_3}\right) = 0.6 \times 2\pi 1000$ . If we wish that the design be resistant to resistor tolerances, we choose  $\frac{r}{R_3} \ll 1$ . So, we choose  $r = 1\text{k}\Omega$  and  $R_3 = 10\text{k}\Omega$ . This allows us to choose  $R_1 = 7188\Omega \approx 7190\Omega = (6800 + 390)\Omega$ .

Back-calculating the transfer function from the values of the components chosen, we observe that the transfer functions match closely. This verifies the design.

The design was then simulated in SPICE (Refer Appendix B). What we observed was that the output of the other two op-amps was around 22dB higher than the output of the system at low frequencies. This is a limiting factor in the dynamic range of the circuit.

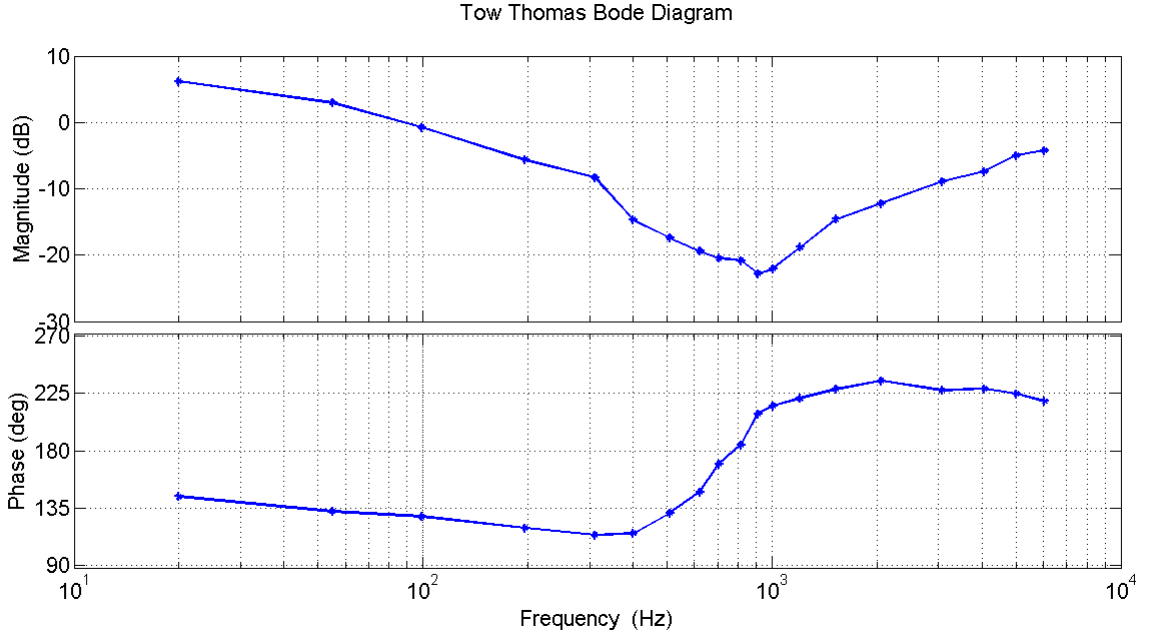


Figure 23: Experimentally measured magnitude and phase responses of second order damped lag network implemented using Tow Thomas biquad topology.

Thankfully, this is not a concern here. We have around 26dB of gain at low frequencies in the H/F lag compensator, and this ensures that the dynamic range of the system is limited only by the rail voltages.

The preceding discussion also gives us some idea about the order of the compensation to be inserted into the system. At the very beginning, we need the L/F lead and the H/F lag compensation to reduce the signal power at low and high frequencies. Then we have the Tow-Thomas biquad with a limited dynamic range at the output. After the Tow-Thomas, we have a lag filter with a large gain. This restores the dynamic range of the signal to the rail voltages.

#### 6.2.5 Characterisation of the Tow-Thomas Biquad

The Tow-Thomas biquad circuit thus designed to implement the second order lag was implemented and tested by characterizing its frequency response. The resulting data is plotted in Fig. 23. We observe a good match between this response and the design (17). Note that the phase response is inverted since the circuit realized is an inverted lag network.

### 6.3 Design of Active First Order Lag/Lead Networks

Active first-order lag/lead networks use a standard topology. The topology is depicted in 24. It is easy to check that the transfer function of the topology is

$$T(s) = \frac{v_o(s)}{v_i(s)} = -\frac{C_1}{C_2} \frac{\left(s + \frac{1}{R_1 C_1}\right)}{\left(s + \frac{1}{R_2 C_2}\right)} \quad (21)$$

To achieve the first order lag network with transfer function  $5 \frac{s+2\pi 4000}{s+2\pi 1000}$ , we choose  $R_1 = 1.2k\Omega$ ,  $R_2 = 24k\Omega$ ,  $C_1 = 33nF$  and  $C_2 = 6.8nF$ .

SPICE simulation results for the Tow-Thomas biquad and the HF lag have been attached in Appendix B at the end of the report.

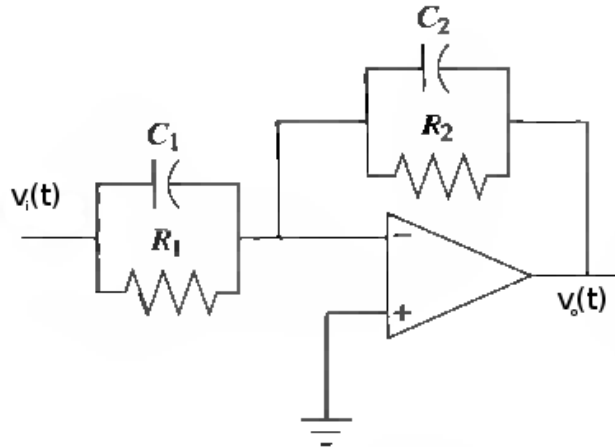


Figure 24: A Topology for an Inverting Active First Order Lag or Lead Network

#### 6.4 System testing and issues

With the circuits for the two parts of the compensation network implemented, we tried to evaluate the closed loop system for its noise cancellation and music following characteristics. Two major issues were subsequently observed -

1. A **high frequency howling** was occurring at high volumes on the headphones. The output of the mic pre-amplifier was measured and the frequency of howling was determined to be 5 KHz. This was very likely due to insufficient gain margin at this frequency (5 dB from the design), since the compensation was focused at stabilizing the system at 1 KHz and 3 KHz resonances.
2. The bass components of music input fed to the system were perceived to be heavily distorted. It was realized that this was occurring due to **overdriving of the headphone actuator** at these frequencies, thereby resulting in non-linear operation. The headphones were subsequently tested for voltage levels at which overdriving occurs, i.e. a non-linearity appears in the plant output. This was compared with the output of the compensator driving the headphones. It was decided to reduce the compensator gain by 6 dB. One quick solution tried out was to reduce the compensator ( $C$ ) gain and proportionately increase the pre-amp ( $A$ ) gain. Maintaining the product  $CA$  constant ensures that the noise cancellation level is not compromised. However, as a result, there is a uniform reduction in the sound pressure output of the headphones. Further, this approach only scales down the magnitude response but does not shape it. As a result, overdriving continues to occur at high volumes.

## 7 Modified Compensation Network and System Testing

The problems observed with the primary compensation motivate the need for modifications to the compensation design. We make the following additions to the existing compensator -

1. A **second high frequency lag** to improve the gain margin around 5 KHz by at least 5 dB to overcome the howling at this frequency.
2. A **low frequency lead** to reduce the gain for frequencies below 200 Hz. We decided to lower open loop gain at 100 Hz by 6 dB. The reduction in gain at 100 Hz due to this part of the compensator can be compensated for by increasing the gain of the pre-amp. This ensures that the cancellation figure remains unchanged.

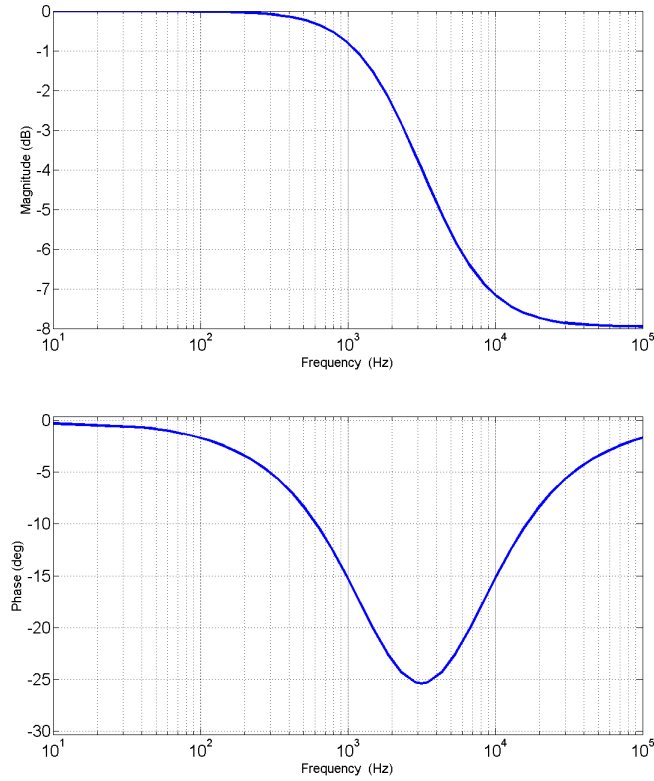


Figure 25: Bode plot of additional first order lag designed to lower gain at frequencies beyond 4 KHz

### 7.1 Inclusion of LF lead and new HF lag

The design procedure for the new HF lag is similar to that of the one designed for the 1-4 KHz. We achieve a 5 dB reduction in gain at 5 KHz (and hence a corresponding improvement in gain margin) and 8 dB reduction at higher frequencies. This was done with  $f_z = 10$  KHz and  $f_p = 4$  KHz. Fig. 25 shows the Bode plots for this network.

For the LF lead system, we keep the desired 6 dB reduction at 100 Hz as a target, and we arrive at the frequencies  $f_z = 50$  Hz and  $f_p = 200$  Hz. Fig. 26 shows the Bode plots for this lead system. We can see that we achieve a 12 dB reduction at low frequencies. The phase response is not too significant considering that the plant in this region is subsequently above  $-180^\circ$ .

These circuits are realized with the standard topology for lag/lead networks discussed previously. The design uses the following component values -

- LF lead  $\frac{s+2\pi 50}{s+2\pi 200}$ ,  $R_1 = 100\text{k}\Omega$ ,  $R_2 = 24\text{k}\Omega$ ,  $C_1 = 33\text{nF}$  and  $C_2 = 33\text{nF}$

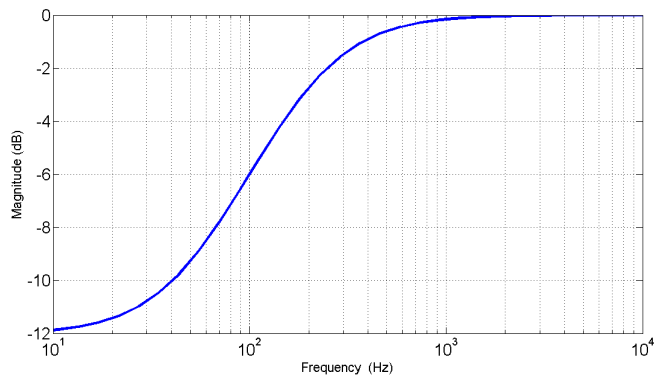


Figure 26: Bode magnitude plot of first order lead designed to lower gain at frequencies below 200 Hz

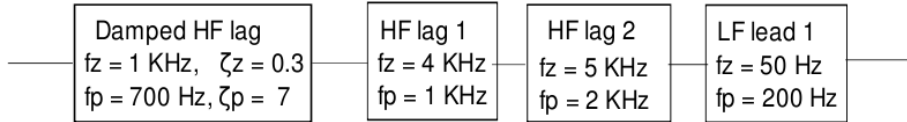


Figure 27: Block diagram of the entire compensation system showing various lag and lead networks

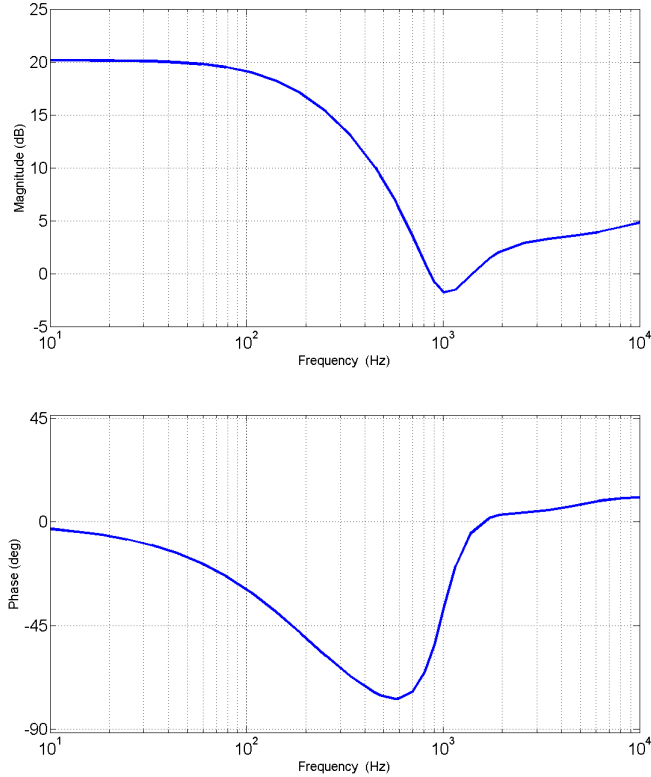


Figure 28: Bode plot of the entire compensation network

- HF lag 2  $\frac{2}{5} \frac{s+2\pi 5000}{s+2\pi 2000}$ ,  $R_1 = 1.8\text{k}\Omega$ ,  $R_2 = 1.8\text{k}\Omega$ ,  $C_1 = 15\text{nF}$  and  $C_2 = 47\text{nF}$ . This gives a lag compensation between 1800Hz and 5800Hz, but we reverify from the simulation that this drift is acceptable.

## 7.2 The cascaded compensator and its characterization

To summarize, Fig. 7.2 presents a block diagram of the entire compensation network. We now examine the cascade compensation design and re-evaluate the stability margins for the forward path system. Fig. 29 compares the compensated and uncompensated plants and shows stability margins for both cases. We observe the following important features -

1. A general reduction in gain beyond the 1 KHz region, which was sought, and specifically, a 22 dB reduction at 1 KHz. We achieve stability margins of around 10 dB at the phase crossover frequencies
2. The phase response is retained almost unchanged, thereby the existing phase margins which are sufficiently robust are not compromised upon.

The schematic for the entire circuit including the complete compensation network, pre-amp and adder is attached in Appendix C. SPICE simulations for individual circuits in the compensation network and that of the entire cascade are also attached in Appendix B.

The entire compensation network was tested for its frequency response. We observe a good match between the experimentally observed response (Fig. 30) and the design. Note that the phase response is inverted due to inverting nature of the circuit realized.

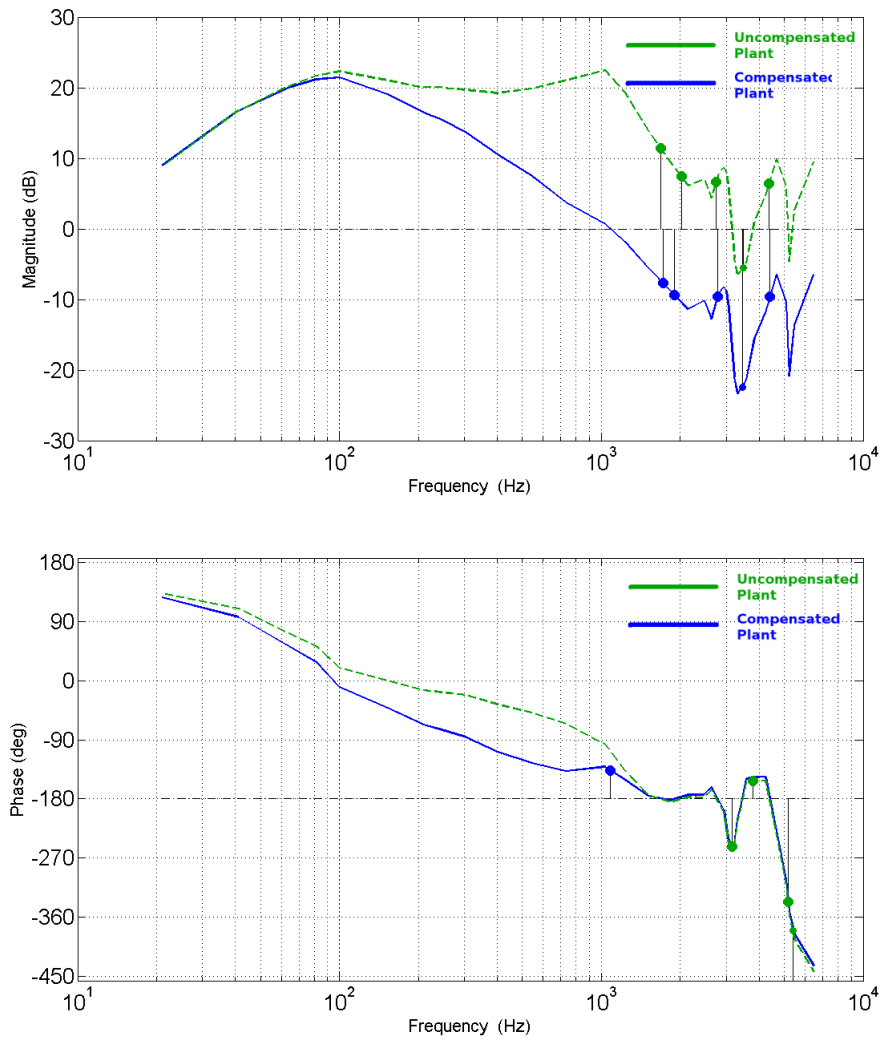


Figure 29: Bode plots comparing the magnitude and phase responses of the uncompensated plant with a gain of 20 dB and the compensated plant

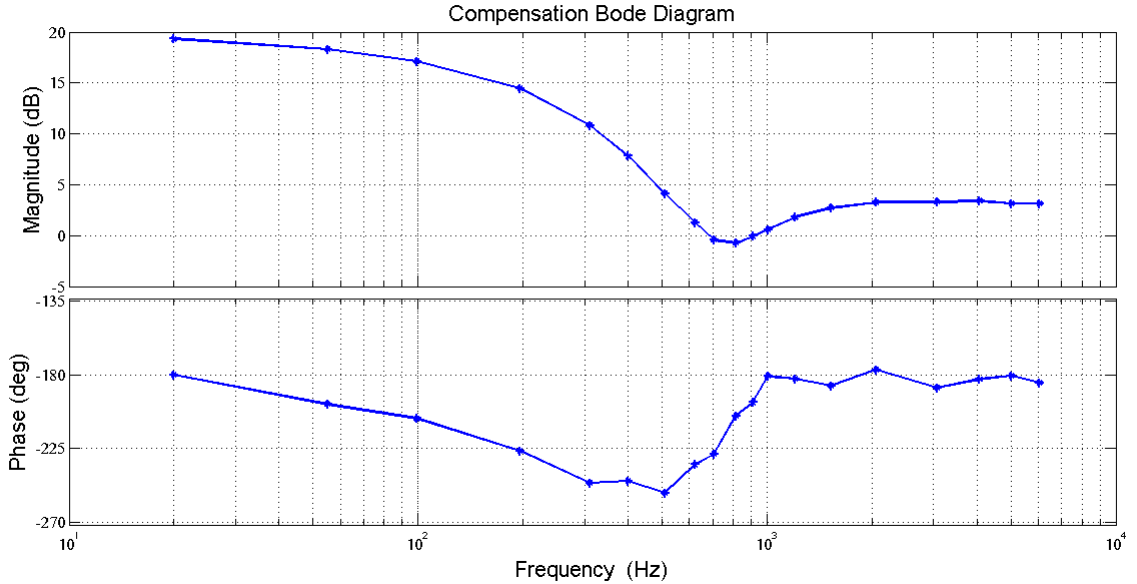


Figure 30: Experimentally measured magnitude and phase responses for the entire compensation network

### 7.3 Evaluation of closed loop frequency responses

Figs. and 31 and 32 show the closed loop frequency responses for the music and noise signals, i.e  $G_{CL}$  and  $R_{CL}$  with the compensation design in place. Note that  $1/|G_{CL}|$  represents the noise cancellation function. We observe the following important features -

1.  $G_{CL}$  has a maximum dip of 22 dB at 100 Hz. This is the theoretically predicted noise cancellation figure at 100 Hz. Subsequently, the cancellation rolls off and reaches 0 dB at 800 Hz.
2. The closed loop magnitude response for the music remains almost unchanged when compared to the open loop plant over the cancellation band. In fact, we observe a flattening of the response at frequencies below 100 Hz, which is actually an improvement over the plant characteristics. We expect this to show in better rendering of bass.
3. It can be seen from the closed loop music phase response that the variation in phase over the cancellation band has been reduced. Compared with that of the original plant (Fig. 4), we observe a halving in the phase variation over 20 KHz - 1 KHz.

### 7.4 Compensator for the right channel

We retain the same compensation design for the right channel plant considering that responses of both channels are not substantially different except for a constant gain factor. This factor is accounted for by adjusting left and right channel pre-amp gains so that equal gains are achieved for both plants.

In addition, we see from the phase response data that the right channel (Ref. Appendix A) is roughly inverted with respect to the left. In order to use the same compensation design, we require an additional inversion. Since we have used up 8 op-amps, that is 2 quad op-amp packages per channel, it would not be a good idea to add an inverter. So, we decided to invert one of the compensation networks.

In theory, any of the compensation networks could be changed to non-inverting, however, we decided to change the low frequency lead network to non-inverting. The topology of a passive low frequency

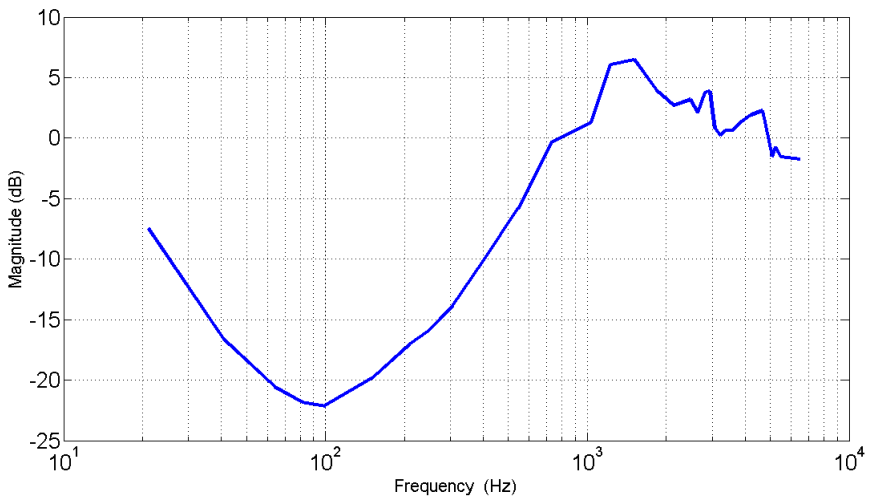


Figure 31: Bode magnitude response plot showing closed loop transfer function for the noise signal

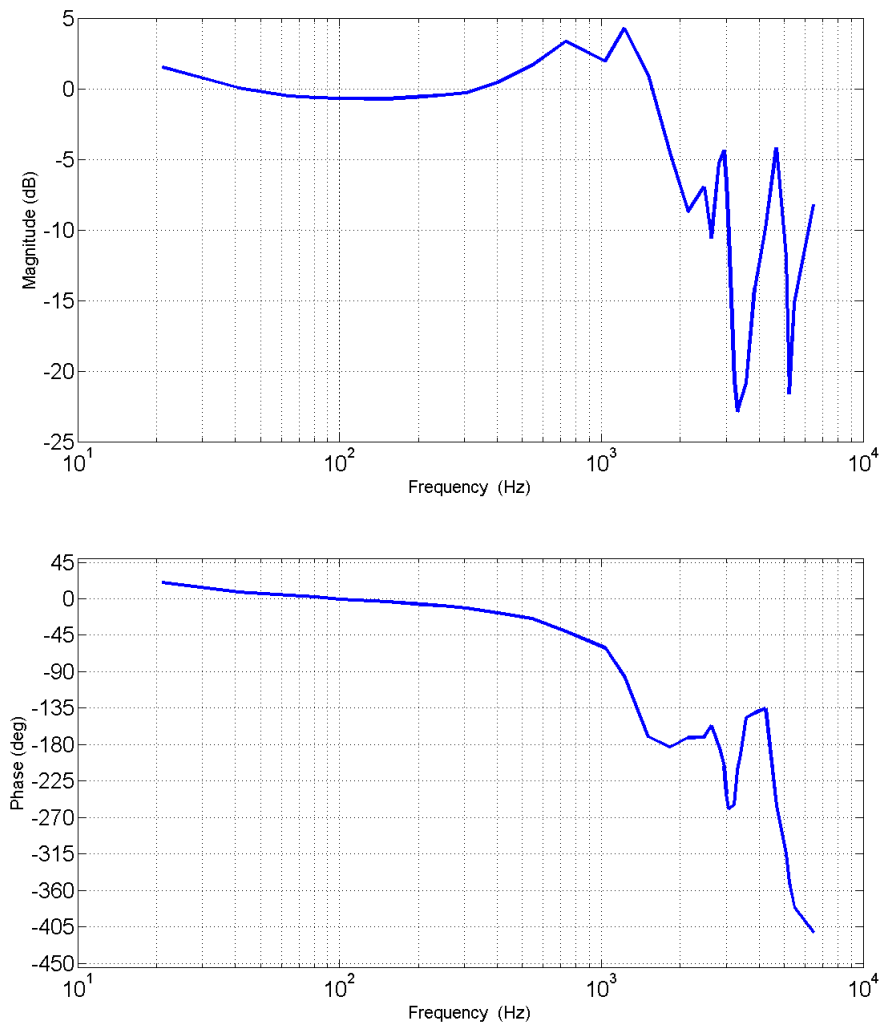


Figure 32: Bode magnitude and phase plots for the closed loop transfer function for music

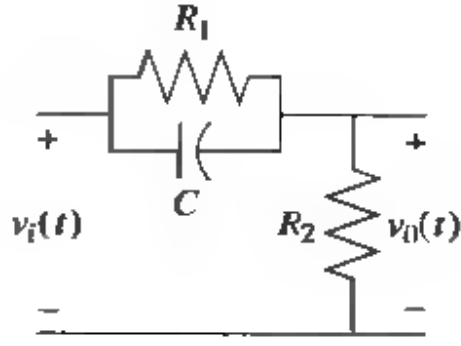


Figure 33: Passive Lag Network Topology

lead network is shown in Figure 33. The transfer function of the lead network is given as

$$T(s) = \frac{v_o(s)}{v_i(s)} = \frac{s + \frac{1}{R_1 C}}{s + \frac{1}{R_1 C} + \frac{1}{R_2 C}} \quad (22)$$

The output of this network is then fed to a unity gain buffer. In this way, the lead network on the right channel differs from the left channel.

## 8 Results and Discussion

In this section, we shall highlight some of the tests we carried out on the complete closed-loop system in order to evaluate its efficacy in terms of input following and amount of noise attenuation. In the first experiment we shall evaluate the amount of noise cancellation obtained vs. frequency by using external speakers to generate an ambient noise tone. Through the second experiment, we wish to identify the response of the music input to the closed loop system and see if this tallies well with the original plant.

### 8.1 Noise Cancellation Response Measurements

In this experiment, we play out a tone of 100Hz - 1000 Hz, in steps of 100 Hz, from a speaker connected to the computer and observe the level of noise cancellation that is obtained for the closed-loop system. We compare against the case in which the line to the speaker is disconnected and the only attenuation that is received is passive attenuation. Thus, our control experiment consists of just passive attenuation, and taking the ratio of the two should give us the effect of just the active noise canceling system.

One run of the experiment is undertaken for each frequency of the ambient tone source. Each run lasts for 10 seconds of sound recording. We conduct each run of the experiment in two parts. In the first part ( $\approx 5$  sec), we have the system in closed-loop with the output of the mic pre-amp being fed via a line-in jack to the computer for further analysis. Thus, the first part of the run corresponds to the **noise attenuating** situation. The transfer function between the noise ( $N(s)$ ) and the output ( $L(s)$ ) is:

$$R'_{CL}(s) = \frac{MAH_2}{1 + PC} \quad (23)$$

In the second part, we disconnect the headphone jack from the rest of the circuit, so that the feedforward is broken. In this situation, the only measured noise is whatever is reaching the mic pre-amp and getting fed to the computer via the line-in jack:

$$R'(s) = MAH_2 \quad (24)$$

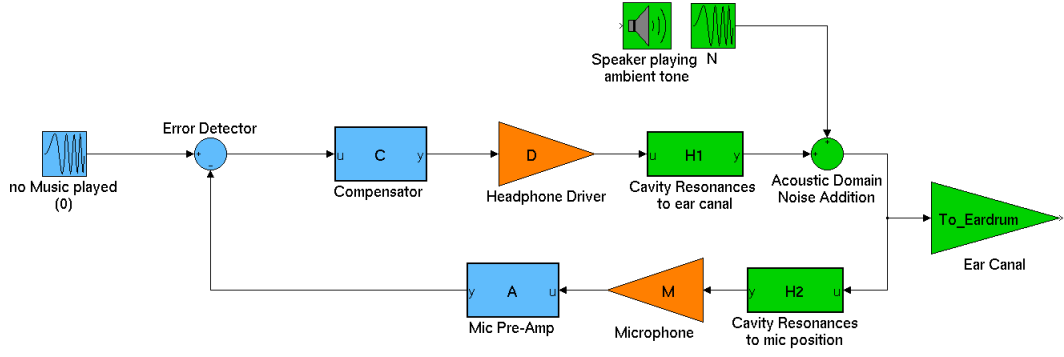


Figure 34: A schematic diagram for the connection of the blocks during the noise cancellation experiment. The input is set to zero, as we wish to qualitatively perceive the effect of noise cancellation - and measure waveforms for the canceling and non-canceling periods.

Thus, we find that the ratio of the two transfer function directly gives us the closed loop noise attenuation function  $R_{CL}(s)$ . We have made an assumption in this analysis that the transfer function of the line-in jack to the computer is unity, or the same for both parts of the same run. This would be a reasonable assumption to make. The upshot is that the ratio of the amplitudes for the attenuating and non-attenuating parts directly gives us the noise attenuation ratio at that particular frequency, thus enabling us to take a frequency characterization of the amount of noise cancellation provided.

Some time-domain graphs of this experiment are attached (measured using the software audacity), around the 5 second switch-over time between attenuating and non-attenuating modes.

In the above graphs, there is a pronounced low frequency variation riding on the tone which can be observed to be getting cancelled in the attenuating mode. This is a further indication of the fact that the system is able to deal with low frequency variations quite well. Indeed, this is in agreement with the predictions made regarding the noise cancelling behaviour from the plant bode plot and the compensator transfer function. We repeated this experiment for several frequencies, and the data we obtained are presented below.

In the analog circuit implementation of the system, we have been using standard tolerance(10%) resistor and capacitor values and approximate values when exact values have not been possible. This would induce an error of 10 – 20% in the filter parameters we made. Also, for the two plant characterisations, we observed a marked variability in the plant gain due to the variation of the ear-cavity. This is an issue often found in the literature on active noise cancellation headsets: the variability of the plant is often an important problem, specially for adaptive systems. Also, the positioning of the error-detecting microphone is an important issue, and could lead to different and changing ear cavity responses depending on slight changes in orientation. (Ref. 3, Ref. 8)

## 8.2 Music Response Characterisation

In the final count, we are not only interested in the noise cancellation, but also in the response of the closed loop system to the music. One of the goals in using a feedback control system was to ensure that the high open loop gain also leads to a flat closed loop response of the plant with respect to the music, since if the open loop gain is high, we do approach a constant gain for the overall closed loop system. A comparison of the plant and the open loop system is required, in order to determine how the net system has been improved with respect to the music.

In order to do this, a characterisation of the open loop system was set up. A tone was supplied at the music input, and the entire system was connected in feedback. We recorded the output of the mic pre-amp over a range of frequencies. Thus, what we desired to observe is the transfer function with respect to the sound reaching the ear canal:

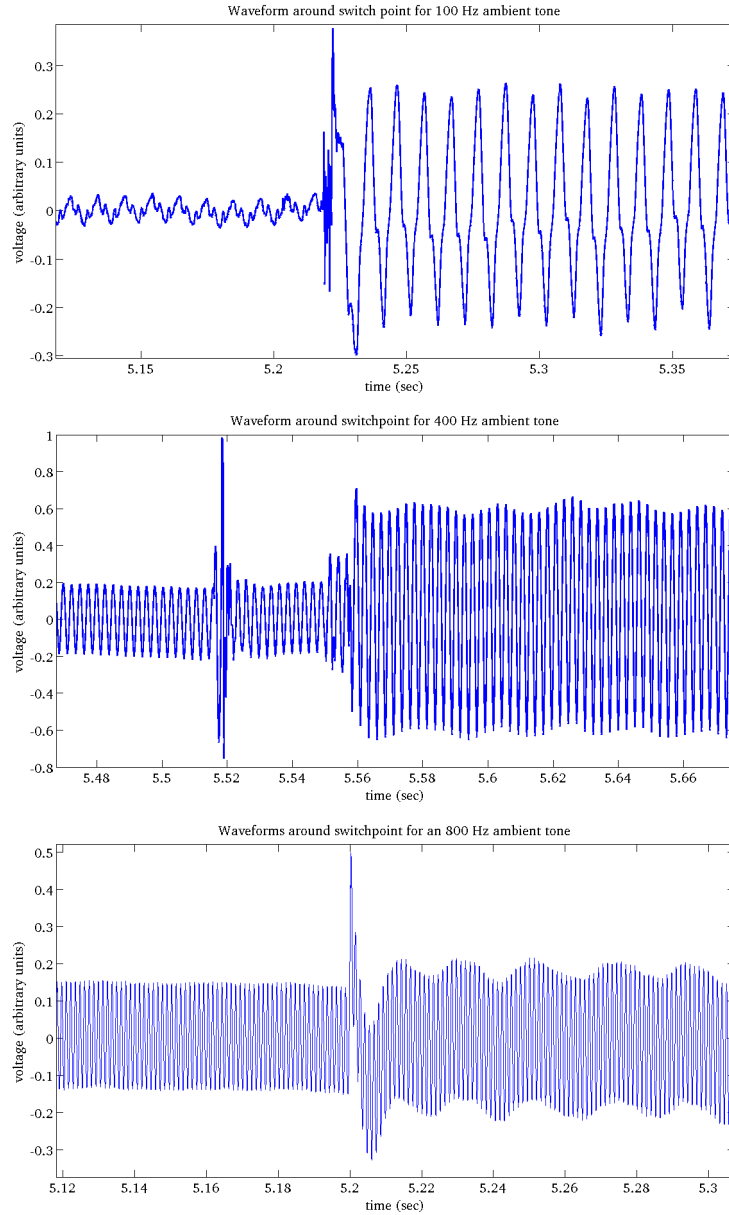


Figure 35: top to bottom: waveforms around the switchpoint for ambient tone frequencies of 100 Hz, 400 Hz and 800 Hz respectively; We compare the ratios of the attenuated and normal signals and see that the noise attenuation transfer function that is measured also qualitatively goes down as frequencies increase. At 100 Hz, there is a cancellation of almost 18 dB, which goes down to 10 dB at 400 Hz and almost 0 dB at 800 Hz.

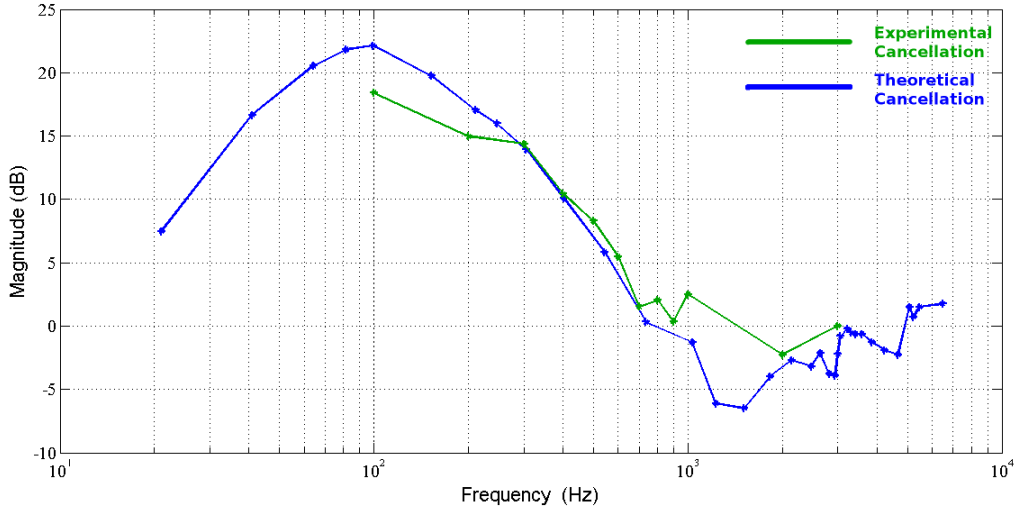


Figure 36: A bode plot of the level of noise cancellation expected from the system, and that actually obtained. blue: expected noise cancellation level from the designed compensator and the plant, green: experimentally measured noise cancellation obtained; we see that the peak noise cancellation at 100 Hz has reduced by about 4-5 dB from the theoretically expected system. Reasons for this could include the variability of the plant, as well as the variability induced due to the resistor and capacitor tolerances.

$$G_{OL}(s) = \frac{DH_1C}{1 + PC} \quad (25)$$

But, we finally end up measuring:

$$G'_{OL}(s) = \frac{PC}{1 + PC} \quad (26)$$

which is the transfer function with respect to the output of the mic pre-amp. The results that follow must be interpreted with the assumption that the feedback loop is essentially behaving as a gain - which is not too far from the truth. Thus, what we observe at the output of the mic pre-amp is a good indication of the music.

A comparison of the open loop plant (without compensator) and the closed loop system is presented below:

As we observe, the response is very flat and leads to a very nice bass response as perceived by the user - leading to a better musical experience over and above the noise cancellation observed. Indeed we see that in implementing this system, we have not only achieved the major goal of noise cancellation - but also an advantage in terms of improving the system over all.

Finally, we will conclude with a discussion of some of the issues with the system and possible improvements that can be made to our project:

- **Howling:** If the closed loop is unstable, we would obtain a high intensity howling noise - in essence the circuit would act like an oscillator, and totally fail in its functionality. One way to prevent this is to keep the open loop gain low enough that the system behaves in a stable manner - though this would not grant us a high amount of noise cancellation - this is a fundamental trade-off to the system.
- **Transient Response:** The microphone pre-amplifier circuit we use is a high pass filter with a pretty low frequency cut-off of around 0.33 Hz. This would lead to a high time constant of around 3 seconds. Thus, on adjusting the headphones, we observe a series of clicks, and a momentary reduction in noise cancellation - after which the noise cancellation becomes perceptible. The high pass filter at the mic pre-amp is for removing the DC offset at the mic output, so we have not come across a way to rectify this issue.

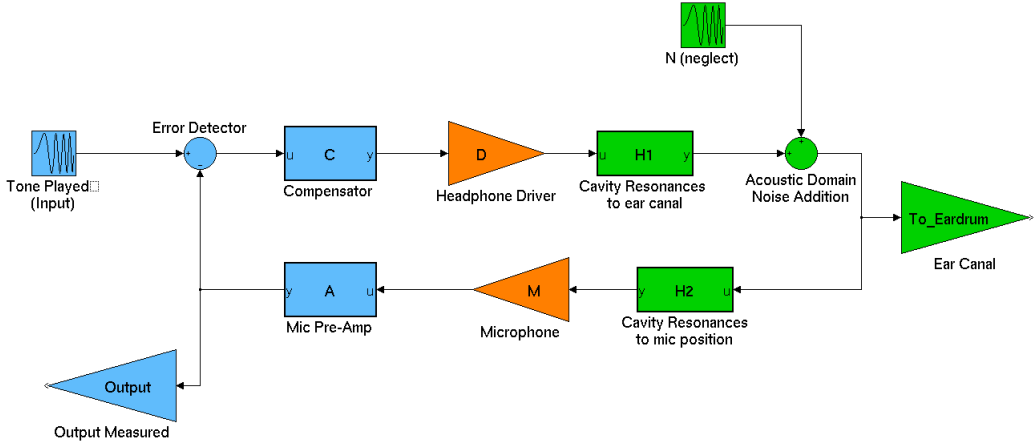


Figure 37: A schematic showing the experiment used to measure the closed loop system characteristics. We would expect the control system to try to maintain a gain of unity, by the basic nature of negative feedback.

- **Change in Plant:** We characterized the left and right channels and found their frequency responses to be quite similar - and thus decided to use the same basic topology of compensation circuitry for both the channels. But it might happen that with time, both the plants may drift in differing ways and lead to entirely different responses. One way to deal with this would be to design a highly robust control system, with sufficient margins and gains so as to deal with uncertainties in the plant. Such techniques are a focus of study in automatic control.
- **Level of Noise attenuation:** The highest level of noise attenuation perceived with this system was around 17-18 dB at 100 Hz, in a very quiet environment. But, this figure keeps changing under different testing conditions - going as low as 12 dB under some cases. This kind of a variability is again due to the changing plant. One possibility under such a condition would be to go for a hybrid system which would bank upon the analog internal control loop to mitigate the variations due to changes in the plant, and an external digital control loop, which would give a high degree of noise cancellation.

## 9 Conclusion

During the course of this project, we have explored two distinct methods of achieving active noise cancellation using analog circuits - feedback and feedforward. The feedforward system comes with inherent limitations of being non-automatic and poor noise cancellation levels. This motivated the shift towards a feedback approach. The feedback system was based on stabilization using a cascade compensator - this idea was originally proposed in a patent by Bose. The work in this part of the project essentially involved the aspects of designing a control system for input following and disturbance rejection. Starting off with a characterization of the plant, we designed a suitable compensation network to stabilize the plant and achieve a maximum noise cancellation level of 20 dB and operating in a cancellation bandwidth of 100 Hz - 1 KHz. The feedback system thus designed was tested for its closed loop frequency responses for music and noise, and we found the results to match theoretical design predictions within the limits of plant variation. We recorded a maximum reduction in noise level of 17 dB at 100 Hz. The closed loop music response was found to be improved over the plant in terms of a flatter response for bass inputs and a lesser phase variation.

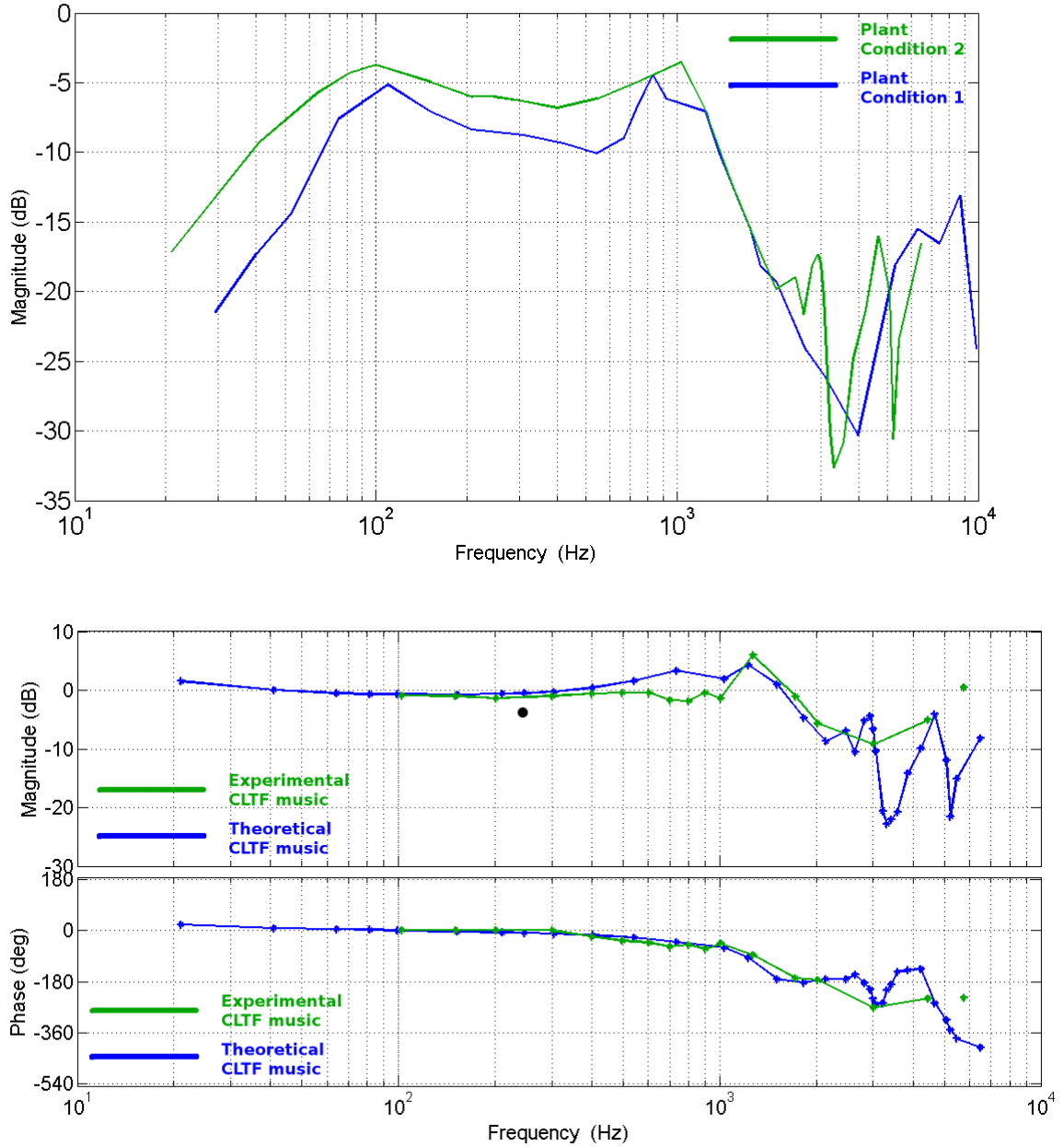


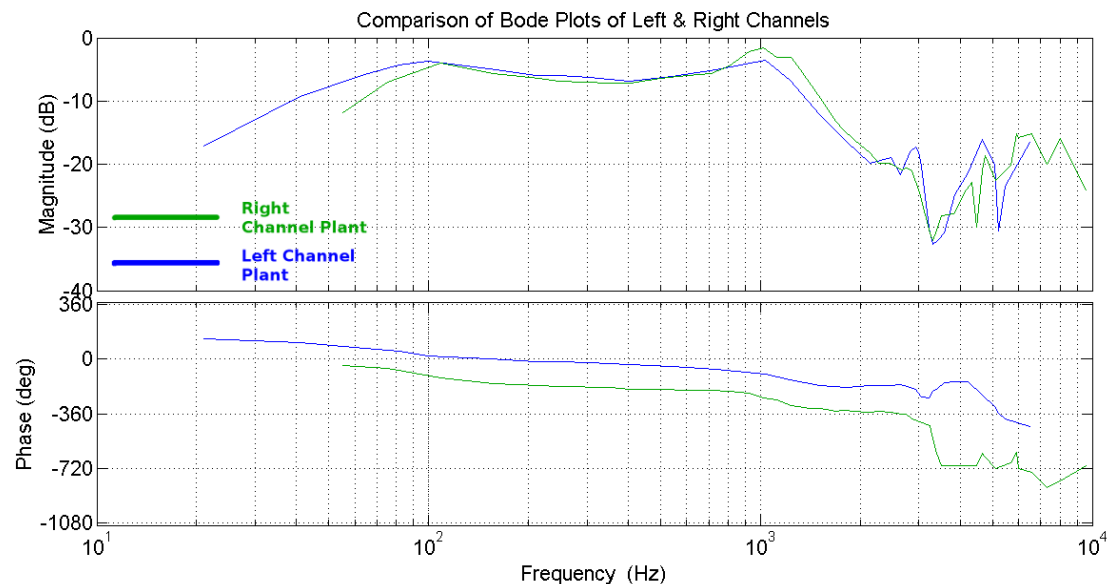
Figure 38: top: The original plant, without any control setup - the blue and green curves correspond to different observation data - but the irregular frequency response of both the curves is quite marked, which is what needs to be emphasized here. middle: The compensated, closed-loop plant, showing a much flatter magnitude response (blue: theoretical, green: obtained experimentally) bottom: The phase response is quite flat too - and may be compared with the original phase response - which falls off very sharply.

## References

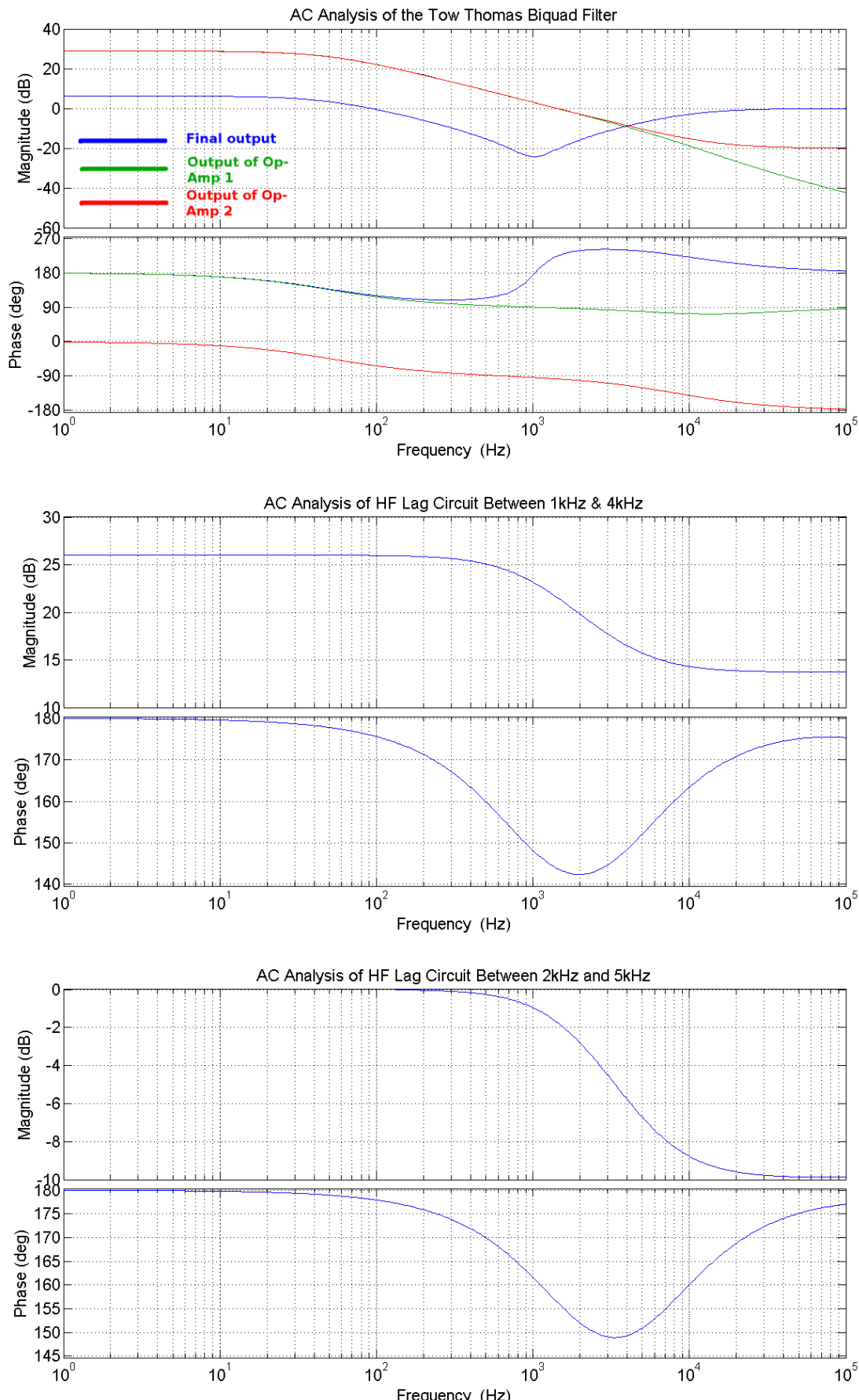
- [1] *Circumaural headphones*, [http://en.wikipedia.org/wiki/Circumaural\\_headphones](http://en.wikipedia.org/wiki/Circumaural_headphones)
- [2] S. Wu, *Noise Canceling Headphones*, Department of Electrical and Systems Engineering, Washington University in St. Louis, 2008
- [3] Ying Song, Yu Gong, and Sen M. Kuo, *A Robust Hybrid Feedback Active Noise Cancellation Headset*, IEEE Transactions on Speech and Audio Processing, Vol. 13, No. 4, July 2005
- [4] Amar Bose, *Headphoning*, US Patent No 4,455,675, 1984
- [5] <http://noise-cancelling-headphones-review.toptenreviews.com/>, *Review of Active Noise Canceling Headphones*
- [6] Sen M Kuo, Sohini Mitra, Woon-Seng Gan, *Active Noise Control System for Headphone Applications*, IEEE Transactions on Control Systems Technology, Vol. 14, No. 2, March 2006
- [7] T. A. Hamilton, A. S. Sedra, *A Single-Amplifier Biquad Active Filter*, IEEE Transactions on Circuit Theory, July 1972
- [8] A. S. Sedra and Smith, *Microelectronic Circuits*, 5th Ed., Oxford University Press
- [9] Norman S. Nise, *Control Systems Engineering*, 5th Ed., John Wiley & Sons, 2009

# Appendices

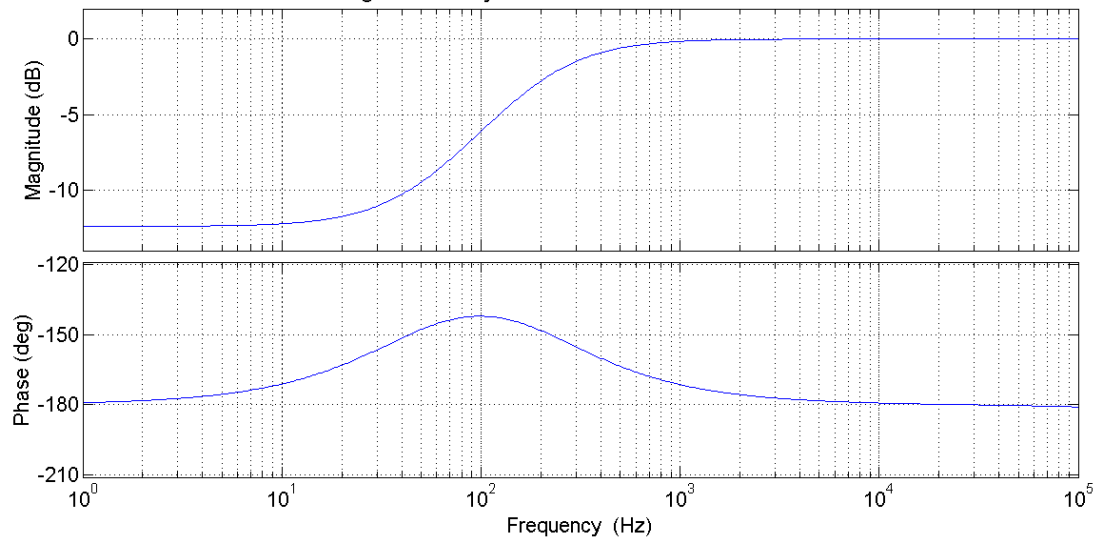
## A Right channel frequency response characteristics



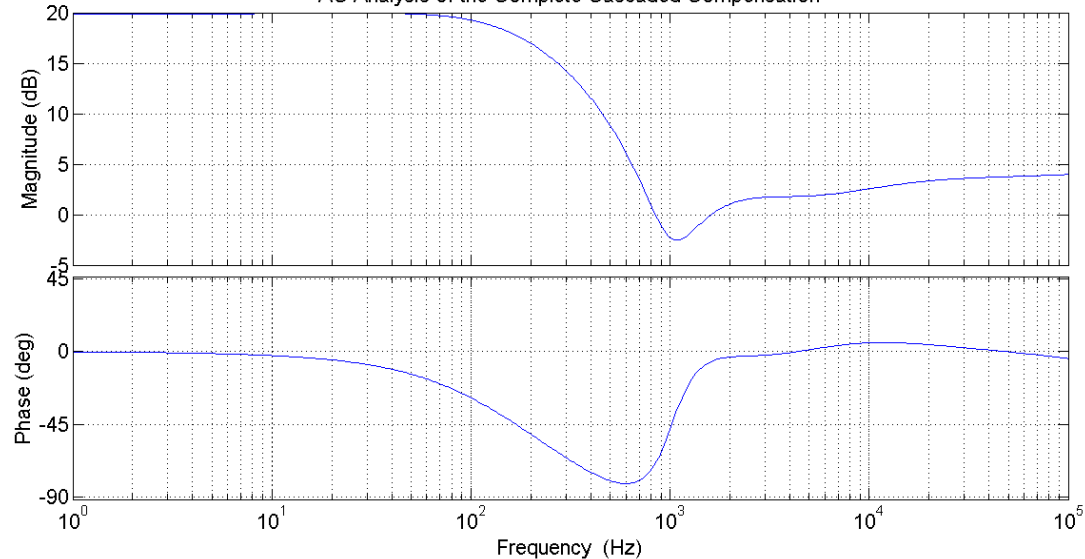
## B SPICE simulation results



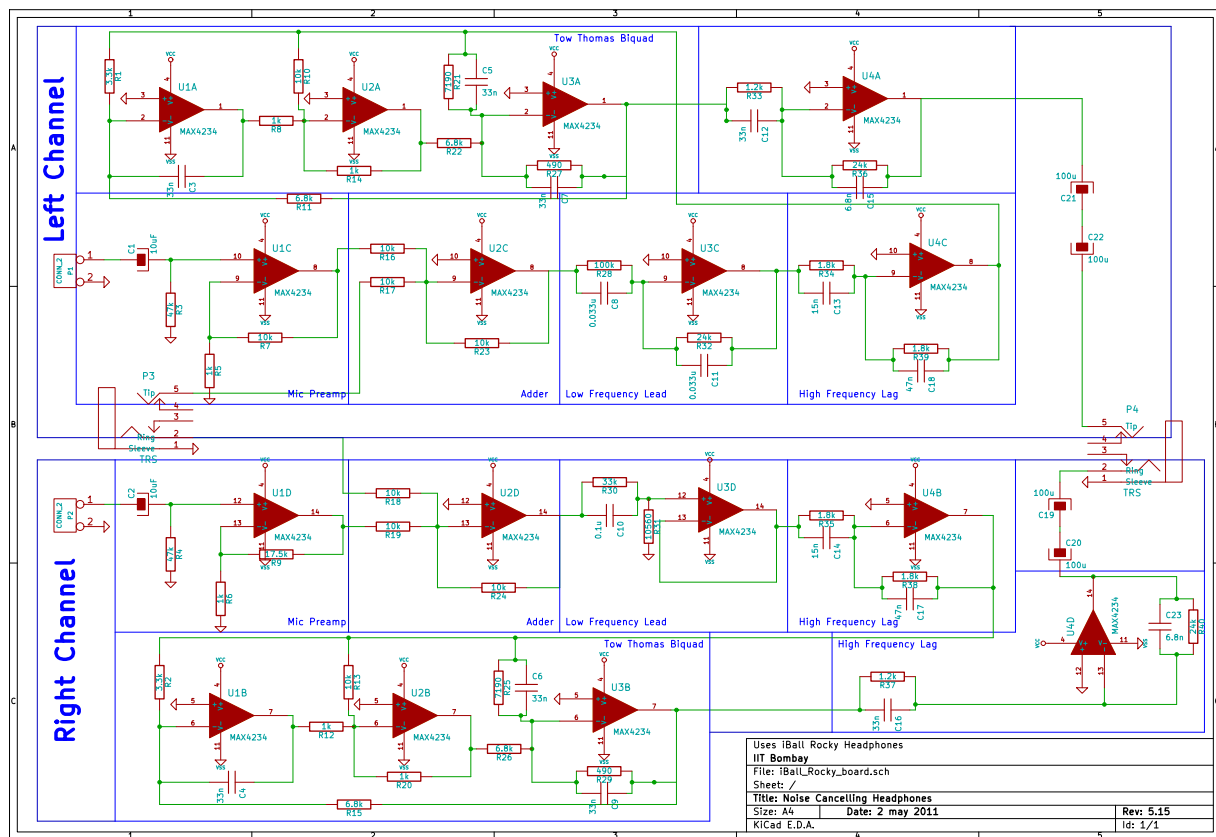
Bode Diagram AC Analysis of Lead Circuit Between 50Hz & 200Hz



AC Analysis of the Complete Cascaded Compensation



## C Complete circuit schematic



## D Final circuit

